© 2019. Published by The Company of Biologists Ltd | Journal of Cell Science (2019) 132, jcs232637. doi:10.1242/jcs.232637

RESEARCH ARTICLE

# Hmgcr promotes a long-range signal to attract *Drosophila* germ cells independently of Hedgehog

**Kim Kenwrick[1], Amrita Mukherjee[2] and Andrew D. Renault[1,*]**

## ABSTRACT

During development, many cell types migrate along stereotyped routes determined through deployment of cell surface or secreted guidance molecules. Although we know the identity of many of these molecules, the distances over which they natively operate can be difficult to determine. Here, we have quantified the range of an attractive signal for the migration of *Drosophila* germ cells. Their migration is guided by an attractive signal generated by the expression of genes in the 3-hydroxy-3-methyl-glutaryl-coenzyme A reductase (Hmgcr) pathway, and by a repulsive signal generated by the expression of Wunens. We demonstrate that the attractive signal downstream of Hmgcr is cell-contact independent and acts at long range, the extent of which depends on Hmgcr levels. This range would be sufficient to reach all of the germ cells for their entire migration. Furthermore, Hmgcr-mediated attraction does not require Wunens but can operate simultaneously with Wunen-mediated repulsion. Finally, several papers posit Hedgehog (Hh) as being the germ cell attractant downstream of *Hmgcr*. Here, we provide evidence that this is not the case.

**KEY WORDS: *Drosophila*, Germ cell, Migration, Hmgcr, LPP, Chemoattraction, Paracrine, Wunen, Hedgehog**

## INTRODUCTION

Cells are often on the move. Microorganisms migrate to find nutrients or a suitable host. Cells in developing embryos can be swept around via large morphogenetic movements, or move either individually or as small collectives of cells pushing through and between tissues. Cells find their way by detecting secreted or cell surface molecules that act as either chemoattractants or chemorepellants. Chemoattractants may be secreted by destination tissues and also by cells along the migratory route that act as intermediate targets. Localised destruction or uptake of chemoattractants are often important for shaping these gradients, as well as encouraging cells to leave the intermediate staging points (Yu et al., 2009; Boldajipour et al., 2008). Cells may also use multiple chemoattractants simultaneously, such as in the case of border cells in the *Drosophila* ovary (Duchek and Rorth, 2001; Duchek et al., 2001).

One cell type whose migration has been studied extensively is the primordial germ cells, the cells that give rise to the gametes in adults. They are formed early in development and migrate during embryogenesis to the gonad in many model organisms (Barton et al., 2016). Their prominence as a model for cell migration arises from their importance for species continuation, ease of identification by morphology, position and gene expression profile, and highly stereotyped migratory routes.

*Drosophila* primordial germ cells initially moved owing to gastrulation rearrangements from their site of formation at the posterior pole into the posterior midgut pocket. Migration begins with the germ cells pulling away from each other and traversing the posterior midgut (Seifert and Lehmann, 2012) (Fig. 1A, stage 10). They move towards the dorsal side of the midgut epithelium and enter the overlying mesoderm, partitioning bilaterally (Sano et al., 2005; Fig. 1A, stage 11). In the mesoderm they associate with the somatic gonadal precursors (SGPs) (Fig. 1A, stage 12), at which point their migration ceases, and together they coalesce to form the embryonic gonad (Boyle and DiNardo, 1995; Fig. 1A, stage 14).

Genetic screens in *Drosophila* have identified two important enzymatic pathways for germ cell migration. The first comprises enzymes of the 3-hydroxy-3-methylglutaryl coenzyme A (Hmgcr) pathway which catalyses the conversion of acetyl groups to the isoprenoids farnesyl- and geranyl geranyl-pyrophosphate, which are used for protein prenylation, as well as being precursors for other lipids (Bellés et al., 2005). Mutations in the *Drosophila Hmgcr* gene [also known as *columbus* (*clb*)] cause germ cells to scatter over the posterior of the embryo (Van Doren et al., 1998). Hmgcr is expressed broadly in the mesoderm before becoming enriched in just the mesodermally derived target tissue, the SGPs (Van Doren et al., 1998). Ectopic expression of Hmgcr, in tissues such as the CNS or the ectoderm, is sufficient to attract a small number of germ cells into the tissue of ectopic expression (Van Doren et al., 1998; Ricardo and Lehmann, 2009). These data suggest that the Hmgcr pathway produces a chemoattractant that attracts the germ cells to the SGPs (Fig. S1).

Some studies report that Hedgehog (Hh) is the Hmgcr-dependent germ cell attractant (Deshpande and Schedl, 2005; Deshpande et al., 2001, 2013). However, Hh itself is not prenylated (Eaton, 2008) and the ability of Hh to attract germ cells has not proven reproducible (Renault et al., 2009). Therefore, the identity of the chemoattractant molecule downstream of Hmgcr remains controversial.

The second pathway involved in *Drosophila* germ cell migration comprises two enzymes, Wunen and Wunen2 (encoded by *wun* and *wun2*), hereafter collectively referred to as Wunens. The Wunens are lipid phosphate phosphatases (LPPs), integral membrane enzymes that can dephosphorylate and internalise extracellular lipid phosphates (Sigal et al., 2005). The Wunens are expressed in somatic regions that germ cells do not normally enter and, in their absence, germ cells scatter over the posterior of the embryo (Starz-Gaiano et al., 2001; Zhang et al., 1997). Overexpression of Wunens blocks germ cell entry into the ectopic tissue and induces death of many germ cells (Starz-Gaiano et al., 2001). In a purely phenomenal (but not necessarily a mechanistic) sense, Wunen expression can be thought of as repelling germ cells (Fig. S1). Wunens are also

[1]School of Life Sciences, University of Nottingham, Queen's Medical Centre, Nottingham NG7 2UH, UK. [2]Department of Zoology, University of Cambridge, Downing St, Cambridge CB2 3EJ, UK.

*Author for correspondence (andrew.renault@nottingham.ac.uk)

A.M., 0000-0002-2659-6557; A.D.R., 0000-0003-4313-9726

**Received 1 April 2019; Accepted 31 October 2019**

Journal of Cell Science (2019) 132, jcs232637. doi:10.1242/jcs.232637

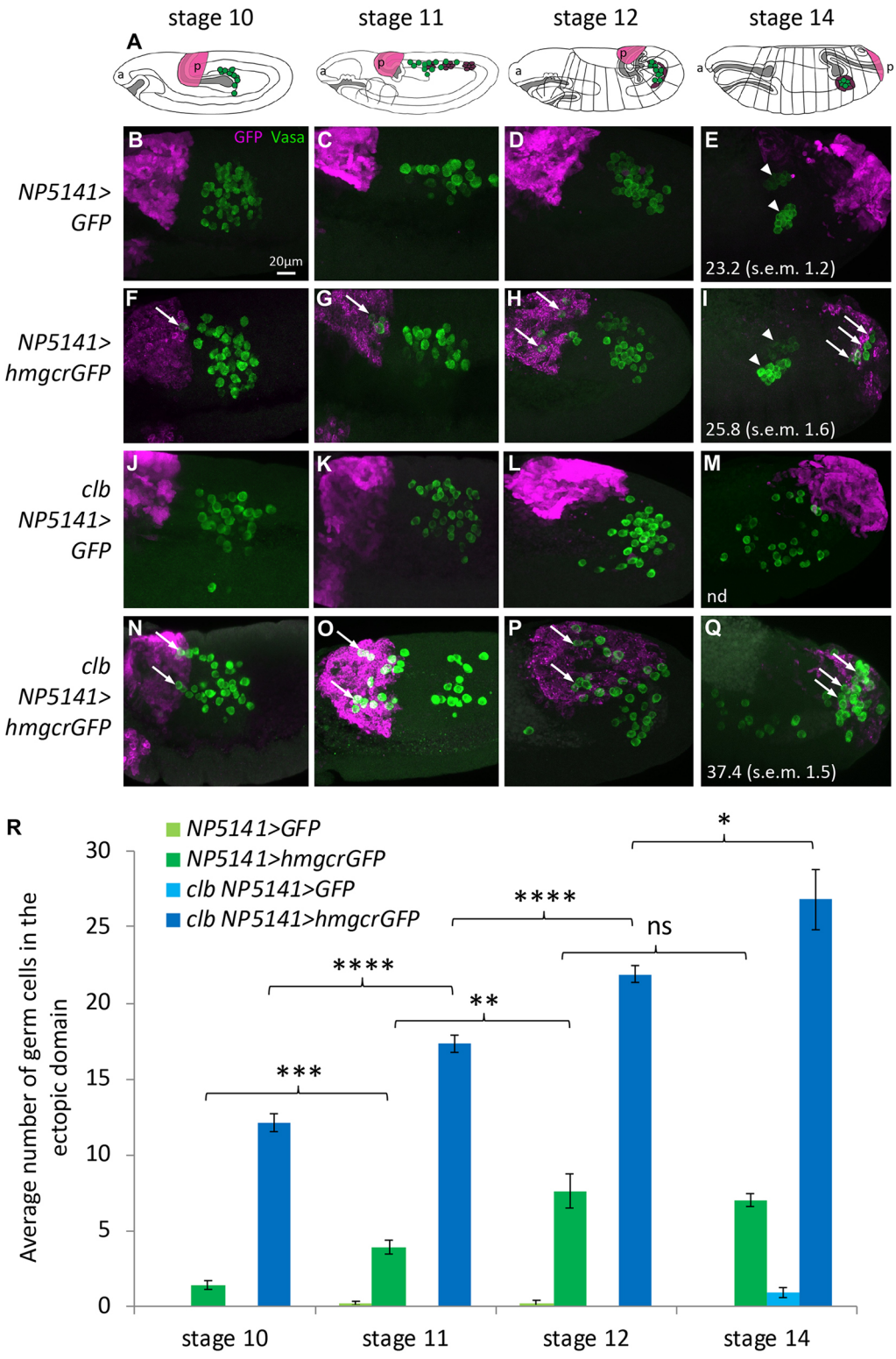


**Fig. 1. *Hmgcr* expressing endogenous and ectopic domains compete to attract germ cells.** (A) Cartoon of lateral views, with anterior (a) left, of *Drosophila* embryos showing germ cells (green) and SGPs (purple) relative to the *NP5141* Gal4 domain in the most posterior parasegment (magenta). Following germ band extension, a stage 10 embryo is folded over on itself so the posterior (p) lies above and slightly to the left of centre. During stage 12, the germ band retracts pulling the posterior to its final position on the right. (B–Q) Maximum intensity projections of lateral views of representative embryos of genotypes: (B–E) *NP5141Gal4/UASGFP*, (F–I) *NP5141Gal4/+;UASHmgcrGFP/+*, (J–M) *NP5141Gal4/UAS GFP;clb$^{11.54}$/clb$^{11.54}$* and (N–Q) *NP5141Gal4/+;clb$^{11.54}$ UASHmgcrGFP/clb$^{11.54}$*, fluorescently stained with antibodies against Vasa to label germ cells (green) and GFP to visualise the ectopic domain (magenta). Arrowheads indicate the position of the embryonic gonads, and arrows indicate germ cells that have been attracted to the ectopic domain. Numbers indicate the mean total number of germ cells at stage 14. (R) Graph showing the mean±s.e.m. number of germ cells in the ectopic domain with $n$=10 embryos scored per genotype (except for *NP5141Gal4/UAS GFP;clb$^{11.54}$/clb$^{11.54}$* for which at stage 11 and 12, three and four embryos were scored, respectively). *$P$<0.05; **$P$<0.01; ***$P$<0.001; ****$P$<0.0001; ns, not significant (two-tailed Student's $t$-test).

Journal of Cell Science (2019) 132, jcs232637. doi:10.1242/jcs.232637

expressed on germ cells themselves (Hanyu-Nakamura et al., 2004; Renault et al., 2004) and this leads to germ-cell–germ-cell repulsion that may be responsible for their initial dispersal out of the posterior midgut (Renault et al., 2010; Fig. S1).

The prevailing idea is that Wunens act to remove an extracellular lipid phosphate attractant (Renault et al., 2004). Although this molecule has not been identified for *Drosophila*, in the ascidian *Botryllus schlosseri*, sphingosine 1-phosphate (S1P) can direct germ cell migration (Kassmer et al., 2015). S1P is an *in vitro* substrate for LPPs (Roberts et al., 1998) raising the possibility that S1P, or a related molecule, acts as an attractant in *Drosophila*. Recent work has demonstrated that the signal downstream of Wunens is likely perceived by germ cells using Tre1, a G-protein-coupled receptor (GPCR) (LeBlanc and Lehmann, 2017).

The most recently proposed model of germ cell migration supposes that the Hmgcr and Wunen pathways work independently of each other (Barton et al., 2016). SGPs produce a prenylated germ cell attractant via the action of the Hmgcr pathway. This prenylated attractant is perceived by germ cells via an unidentified receptor and acts as an attractant. Wunens act on a different molecule, which also acts as a germ cell attractant, such as extracellular S1P or a related lipid, creating a gradient through its localised destruction (Barton et al., 2016). The Tre1 GPCR on germ cells is responsible for sensing the substrate of the Wunens (LeBlanc and Lehmann, 2017) leaving the identity of the germ cell receptor for the Hmgcr-dependent chemoattractant unknown.

Such a model leaves several open questions. Firstly, do the two chemoattractants operate with similar or different characteristics? Perhaps one is long range to get the germ cells initially moving in the right direction from the midgut while the other acts over a short range to finesse the later migration to the SGPs. Secondly, how do germ cells integrate these two signals? For example, how would germ cells respond when given conflicting guidance information by these two pathways? Perhaps, in this scenario, one pathway is dominant over the other.

Previously, we have shown that Wunens expressed in somatic cells repel germ cells without the need for cell-to-cell contact over at least a distance of 33 µm, implying they regulate a long-range diffusible signal (Mukherjee et al., 2013). In this paper, we have used germ cell response to ectopic *Hmgcr* expression to obtain quantitative information on the range of the Hmgcr-dependent signal. We show that, like Wunens, the Hmgcr-dependent signal also acts at long range and can attract germ cells at distances of up to 51 µm. We have used epistatic analyses to investigate the relationship between the *hmgcr* pathway, *wun* and *hh*. We find that *hh* does not act downstream of *Hmgcr* in attracting germ cells and that Wunens are not essential for Hmgcr-mediated attraction. Finally, we discuss these data in relation to models of germ cell migration that posit one versus two chemoattractants.

## RESULTS

### Ectopic *Hmgcr* expression is sufficient to attract germ cells into the ectopic domain

To address the question of whether *Hmgcr* produces a short- or long-range signal, we wanted to examine the distances that germ cells migrate when entering domains of ectopic *Hmgcr* expression (hereafter termed the ectopic domain). We constructed a tagged UAS *Hmgcr* overexpression construct allowing us to simultaneously attract germ cells and visualise the region of misexpression. Ectopic expression of *HmgcrGFP* was as effective at disrupting germ cell migration as previously described untagged *Hmgcr* constructs, indicating that the HmgcrGFP fusion protein was functional (Fig. S2).

We next wanted to ascertain whether *Hmgcr* expression could attract germ cells into ectopic domains as was suggested previously using CNS and ectodermal Gal4 lines (Van Doren et al., 1998). We used the Gal4 driver line *NP5141* previously used to measure the repulsive forces exerted by the Wunens (Mukherjee et al., 2013). This driver expresses in parasegments 2 and 14. The former is far enough anterior that it is unlikely to affect the germ cells, whereas the latter, at stages 10–11, lies dorsally, but posterior to, where the germ cells would normally migrate (Fig. S2A). We found that *HmgcrGFP* expression in the *NP5141* domain is sufficient to attract germ cells away from their normal migration route and for them to enter the ectopic domain (Fig. 1I,E).

To determine the time during which the germ cells were attracted, we examined the number of germ cells in the ectopic domain at different stages. Germ cells were inside the ectopic domain from stage 10 when germ cells have just crossed the posterior midgut and are starting to enter the mesoderm (Fig. 1B,F). Between stages 10 and 12 there were significant increases in the number of germ cells in the ectopic domain (Fig. 1C–E,G–I,R), indicating that germ cell attraction occurs continually rather than at a discrete time point. However, between stages 12 to 14 there was no significant increase in the number of germ cells in the ectopic domain (Fig. 1R). It is at these stages that germ cells contact the SGPs suggesting that this may curb attraction to the ectopic domain.

### Ectopic and endogenous domains of *Hmgcr* compete to attract germ cells

In the above experiment, the SGPs (which naturally express *Hmgcr*) and the ectopic *Hmgcr* are likely competing to attract germ cells. This may lead us to underestimate the attractive range of the *Hmgcr*-mediated signal because potentially more germ cells would be attracted to the ectopic domain were it not for endogenous SGP *Hmgcr* expression.

To test this hypothesis we expressed *Hmgcr* using the *NP5141* driver in a *columbus* (*clb*)-null background (*Hmgcr* loss-of-function alleles are termed *clb*). The number of germ cells in the ectopic domain was significantly increased compared to the wild-type background at all stages (Fig. 1F–I,N–R). Furthermore, the increase in germ cell number inside the ectopic domain continued past stage 12, unlike in the wild-type background (Fig. 1R). Therefore, germ cells can continue to migrate and be attracted to the ectopic domain even late into embryogenesis in the absence of SGP *Hmgcr* expression.

We conclude, firstly, that ectopic *Hmgcr* does compete with endogenous *Hmgcr* in germ cell attraction and, secondly, that the temporal limit of germ cell attraction in wild-type embryos is due to interaction with SGPs rather than a stage-dependent shut down of the germ cell migratory programme.

### *Hmgcr*-mediated attraction can occur in the absence of somatic Wunens

Given that endogenous *Hmgcr* restricts the number of germ cells that can be ectopically attracted, we wanted to test whether other regulators of germ cell migration also have this effect. We therefore examined germ cell attraction in the background of a deficiency that removes somatic *wun* and *wun2* (hereafter referred to as a *wun* mutant background). In some of the genetic backgrounds used in these experiments a sizeable number of germ cells failed to exit the posterior midgut properly at stage 10 (and presumably could not be attracted to the ectopic domain); therefore, we scored the number of germ cells in the ectopic domain as a percentage of the total of all the germ cells that were outside the midgut or hindgut. The latter number was however sufficiently large enough for all

Journal of Cell Science (2019) 132, jcs232637. doi:10.1242/jcs.232637

genotypes (Fig. 2G) to accurately assess the attractive capacity of ectopic *Hmgcr*.

We found that in a *wun* mutant background, germ cells were still attracted to ectopic *Hmgcr* (Fig. 2D,G). However, unlike what was seen in a *clb* mutant background, which drastically increased the percentage of germ cells that were attracted, there was no significant increase in a *wun* mutant background (Fig. 2B,D,G). This is despite the fact that in *wun* mutants just expressing ectopic GFP some germ cells stray into the posterior of the embryo due to random mismigration (Fig. 2A,G) as previously observed (Mukherjee et al., 2013). We conclude, firstly, that attraction to *Hmgcr* does not require the Wunens but, secondly, that Wunen expression does not limit attraction by ectopic *Hmgcr* in a wild-type background. The latter conclusion is supported by the fact that *wun2* is not expressed in the region between the posterior midgut and parasegment 14 (curly bracket in Fig. S3D).

To determine whether Wunens might limit attraction in a *clb* background, we examined germ cell attraction in the triple mutant

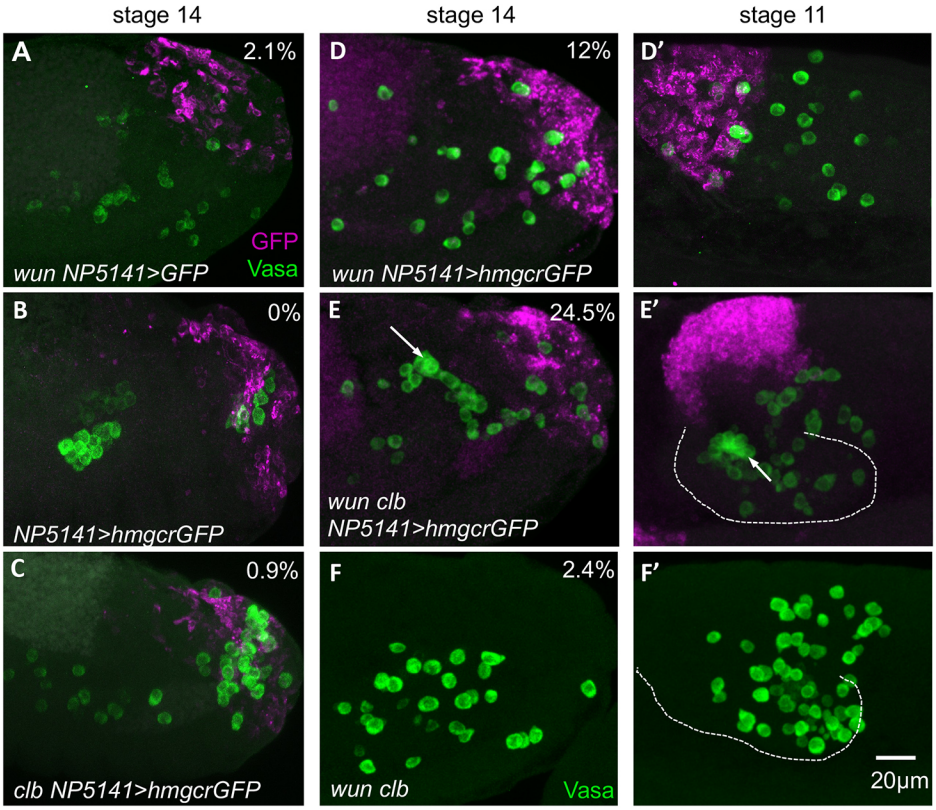


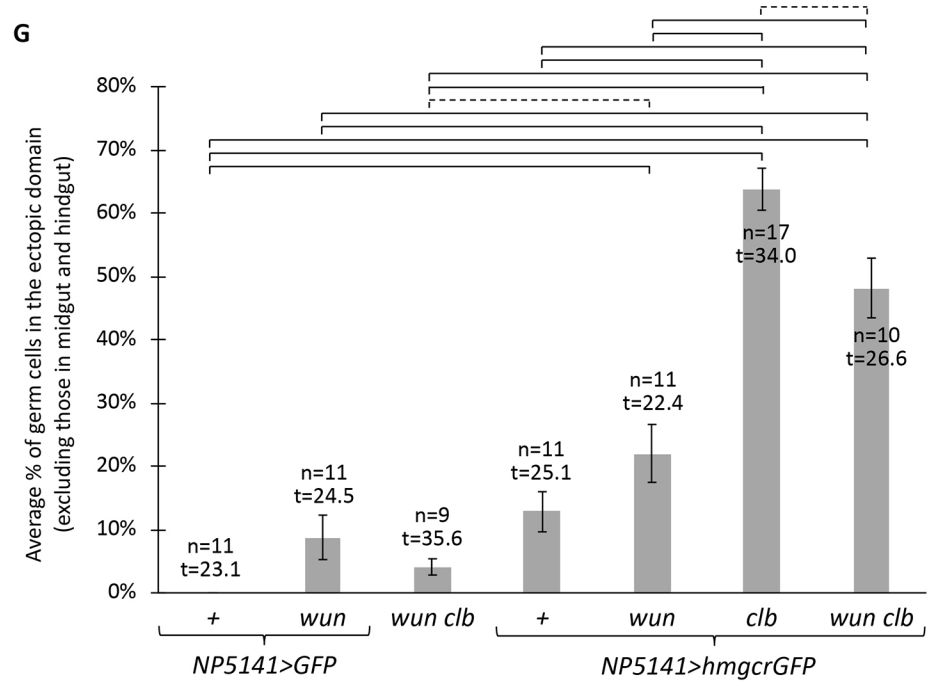


**Fig. 2. Wunen aids *Hmgcr*-mediated germ cell attraction.** (A–F) Maximum intensity projections of lateral views of representative stage 14 embryos (A–F) or stage 11 embryos (D′–F′) of genotypes: (A) *Df(2R)wun$^{GL}$ UASlazGFP/Df(2R)wun$^{GL}$ NP5141Gal4*, (B) *NP5141Gal4/+;UASHmgcrGFP/+*, (C) *NP5141Gal4/+;clb$^{11.54}$ UASHmgcrGFP/clb$^{11.54}$*, (D,D′) *Df(2R)wun$^{GL}$/Df(2R)wun$^{GL}$ NP5141Gal4;UASHmgcrGFP/+*, (E,E′) *Df(2R)wun$^{GL}$/Df(2R)wun$^{GL}$ NP5141Gal4; clb$^{11.54}$ UASHmgcrGFP/clb$^{11.54}$*, (F,F′) *Df(2R)wun$^{GL}$/Df(2R)wun$^{GL}$;clb$^{11.54}$/clb$^{11.54}$* fluorescently stained with antibodies against Vasa (A–F) to label germ cells (green) and GFP (A–E) to visualise the ectopic domain (magenta). LazGFP was used as a control protein for labelling the ectopic domain in A. Arrows point to an elongated cluster of germ cells that have failed to disperse and move out of the midgut but instead are located towards the hindgut (E′) and presumably have become 'stuck' there at later stages (E). Dashed lines indicate outer boundary of posterior midgut. Percentages are the percentage of germ cells that are present in the hindgut at stage 14 (number of embryos scored is the same as in G, for F this is nine embryos). (G) Graph showing the mean±s.e.m. number of germ cells in the ectopic domain in stage 13–14 embryos as a percentage of all germ cells, excluding those that are in the midgut and hindgut (which presumably cannot move into the ectopic domain due to the epithelial barrier). Means that are significantly different are indicated (one-way ANOVA with Tukey's HSD Test, $P<0.01$ for solid lines, $P<0.05$ for dashed lines). All other pairwise comparisons show no significant difference. *n*=embryos scored per genotype. *t*=mean total germ cell number (excluding those in midgut and hindgut). For *wun wun2 clb* mutant embryos the number of germ cells in the ectopic domain was estimated using their distance from the embryo posterior (see Materials and Methods).

Journal of Cell Science (2019) 132, jcs232637. doi:10.1242/jcs.232637

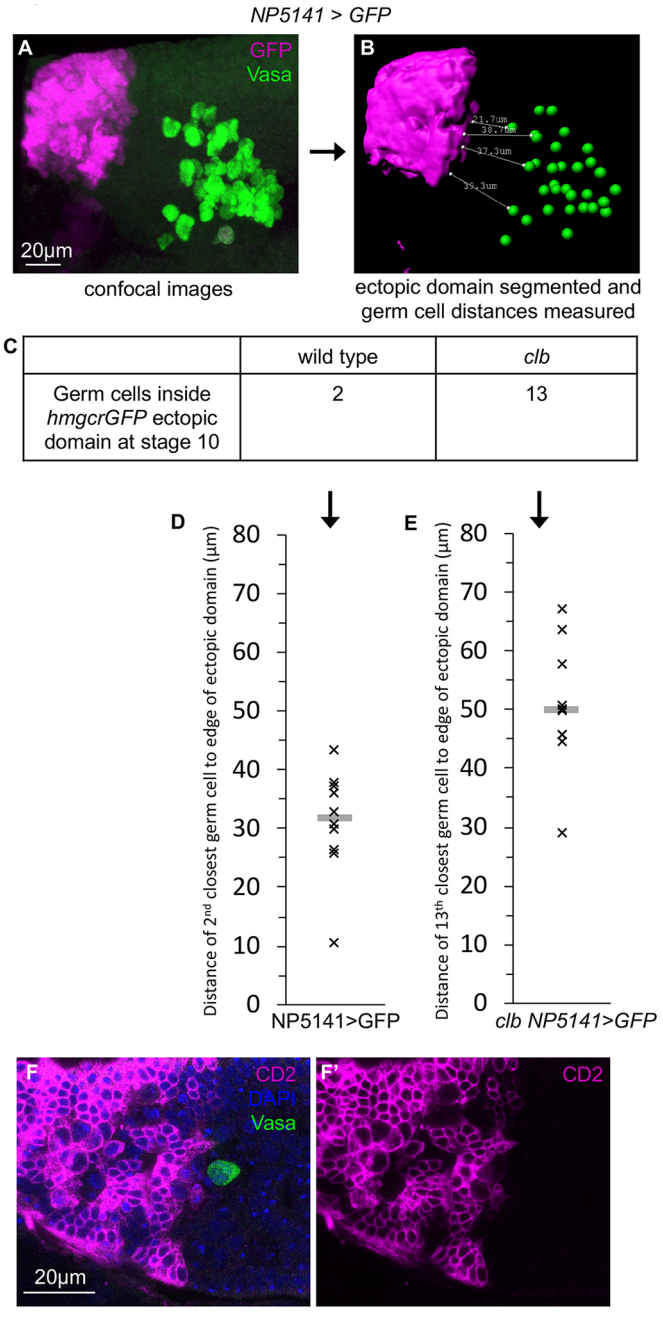


**Fig. 3. Hmgcr mediates a long-range signal.** (A) Maximum intensity projection of a lateral view of a representative *NP5141Gal4*/*UASGFP* stage 10 embryo fluorescently stained with antibodies against Vasa to label germ cells (green) and GFP to visualise the ectopic domain (magenta). (B) Representation of embryo in A after segmentation of the ectopic domain (magenta surface), assignment of germ cell positions (green spheres) and automatic measurement of distances between germ cell and ectopic domain boundaries (white lines, only measurements for the four germ cells closest to the ectopic domain are shown for clarity). (C) Table showing average number of germ cells inside the *Hmgcr*-expressing ectopic domain at stage 10 (taken from Fig. 1R) in a wild-type and *clb* mutant background. (D) Graph showing the distance of the second closest germ cell from a GFP-expressing ectopic domain in a wild-type background. The assumption is that it is these closest two germ cells that would be attracted to a *Hmgcr*-expressing ectopic domain in a wild-type background and thus provides an estimate of the attraction range of ectopic *Hmgcr* when in competition with wild-type expression. (E) Graph showing the distance of the 13th closest germ cell from a GFP-expressing ectopic domain in a *clb* mutant background. The assumption is that it is these closest 13 germ cells that would be attracted to a *Hmgcr*-expressing ectopic domain in a *clb* mutant background and thus provides an estimate of the attraction range of *Hmgcr* without competition from wild-type expression. Grey bars indicate the median distance. Number of embryos scored=10. (F) Single lateral slice through a stage 11 *NP5141Gal4*/*UAS CD2; UASHmgcrGFP*/+ embryo fluorescently stained with antibodies against Vasa labelling the germ cells (green) and CD2 to visualise the plasma membranes of *Hmgcr*-expressing cells (magenta) showing that these cells do not make long projections.

(loss of function for *wun*, *wun2* and *clb*). We found a significant reduction in the percentage of germ cells in the ectopic domain in the triple mutant compared to in the *clb* mutant alone (Fig. 2C,E,G). This reduction was not due to a reduced volume of the ectopic domain in a *wun* background (Fig. S3C). We conclude that repulsion by Wunens does not also limit attraction by ectopic *Hmgcr* in a *clb* background; however, there is some beneficial effect of Wunen expression. This could be due to an effect of Wunen expression either directly on the gradient of the *Hmgcr*-mediated signal or on the positioning of germ cells to ensure they exit the posterior midgut correctly.

In support of the latter hypothesis, we found a large number of germ cells that were in the hindgut at stage 13–14 in the triple mutant background (Fig. 2E). This correlated with a large cluster of germ cells that failed to cross the posterior midgut at stage 10 (Fig. 2E′). Germ cells failing to cross the posterior midgut would normally be found in the midgut at later stages (for example when dominant versions of Rho family GTPases are expressed in germ cells rendering them unable to migrate; Renault et al., 2010). In this case, however, the germ cell cluster was further posterior towards the hindgut (arrow in Fig. 2E′) leading to the germ cells ending up there at later stages. We speculate that without Wunen expression in the posterior midgut (Fig. S1 and arrow in S3D) and without the normal early pan-mesodermal *Hmgcr* expression (Van Doren et al., 1998 and see also Fig. 6A) many germ cells are attracted to ectopic *Hmgcr* before they leave the posterior midgut. These germ cells move towards the hindgut and get trapped there, presumably as they are unable to cross the hindgut epithelium. This is in line with the observation that in *srp* mutants, in which the posterior midgut cells resemble the hindgut, the germ cells become stuck in the midgut (Jaglarz and Howard, 1994; Renault et al., 2010; Reuter, 1994). These data imply that germ cells are able to sense the *Hmgcr*-mediated signal while they are still inside the posterior midgut.

### The *Hmgcr*-mediated signal is long range

We next wanted to make a quantitative assessment of the effective range over which the *Hmgcr*-mediated signal attracts germ cells. Our rationale was to determine how far germ cells are from the ectopic domain when labelled with just GFP because it is at those distances that some germ cells would be attracted when the ectopic domain expresses *HmgcrGFP*.

We focused on stage 10 embryos when the germ cells are first attracted to the ectopic domain. The median germ cell distance from the ectopic domain remains fairly constant between stages 10 to 13 (Fig. S4), therefore we are not overestimating the effective range by focusing on a stage in which the germ cells are particularly close. Firstly, we asked how many germ cells are in the ectopic domain in experimental embryos in which the ectopic domain expresses *HmgcrGFP*. In a wild-type background, this was on average two germ cells (Fig. 1R). Secondly, we took control embryos in which the ectopic domain expressed just GFP and measured the distance of every germ cell to the nearest surface of the ectopic domain, which

Journal of Cell Science (2019) 132, jcs232637. doi:10.1242/jcs.232637

had been computationally segmented (Fig. 3A,B). We recorded the distance of the second closest germ cell based on the assumption that, because *Drosophila* germ cells migrate with a high degree of directionally (figure 1D in Sano et al., 2005; Fig. 4), it would be the two closest germ cells that would have been attracted to ectopic domain if it were expressing *HmgcrGFP*.

The distances of the second closest germ cells were then averaged for the 10 embryos examined (Fig. 3D). In a wild-type background, the second closest germ cell was on average 31 µm (s.e.m. of 2.9 µm) from the ectopic domain, leading us to conclude that the *Hmgcr*-mediated signal is able to attract germ cells over at least this distance.

We next considered whether we might be underestimating the effective range of the *Hmgcr*-mediated signal, because germ cells in wild-type embryos are still subject to competition from endogenous Hmgcr in SGPs (Fig. 1). Therefore, we applied the same methodology to *clb* mutant embryos. In this case, there were on average 13 germ cells in the ectopic domain expressing *HmgcrGFP* in *clb* mutant embryos (Fig. 3C). In a *clb* mutant embryo with the ectopic domain expressing GFP alone, the thirteenth closest germ cell was on average 51 µm (s.e.m. 3.4 µm) from this domain (Fig. 3E). We conclude that the *Hmgcr*-mediated signal is able to attract germ cells over at least 51 µm.

To distinguish whether the long-range signal is a diffusible molecule (and therefore cell-contact independent) versus acts via cytonemes (and therefore cell-contact dependent) we tested whether *Hmgcr* overexpressing cells send out long protrusions. Upon examining embryos with ectopic co-expression of *Hmgcr* and the membrane marker CD2 using the *NP5141* driver, we were unable to visualise any protrusions from cells of the ectopic domain (Fig. 3F,F′, image representative of 10 embryos). Taken together, we conclude that Hmgcr acts to produce a long-range, cell-contact independent (and therefore paracrine) signal in *Drosophila* embryos, which attracts germ cells.

### The range of the Hmgcr-mediated signal is concentration dependent

To test whether the range of Hmgcr-mediated signal is dependent on the levels of Hmgcr expression we tested whether increasing the ectopic *Hmgcr* expression level could increase the number of germ cells attracted to the ectopic domain. We found that while having an extra copy of the *UASHmgcrGFP* transgene had no significant effect, having two copies of both the *NP5141* Gal4 driver and *UASHmgcrGFP* transgenes significantly increased the number of germ cells in the ectopic domain (Fig. 4A–D).

To test whether this effect also occurred in a *clb* mutant we increased the ectopic *Hmgcr* expression level by having two copies of the *NP5141* Gal4 driver in a *clb* mutant background. In such embryos, it was possible to attract virtually all of the germ cells into the ectopic domain (Fig. 4E, compare the number of germ cells outside the ectopic domain to Fig. 1F). The very furthest germ cell was on average 92 µm ($n$=10, s.e.m. 4.2 µm) from the ectopic domain upon crossing of the posterior midgut at stage 10 in *clb*

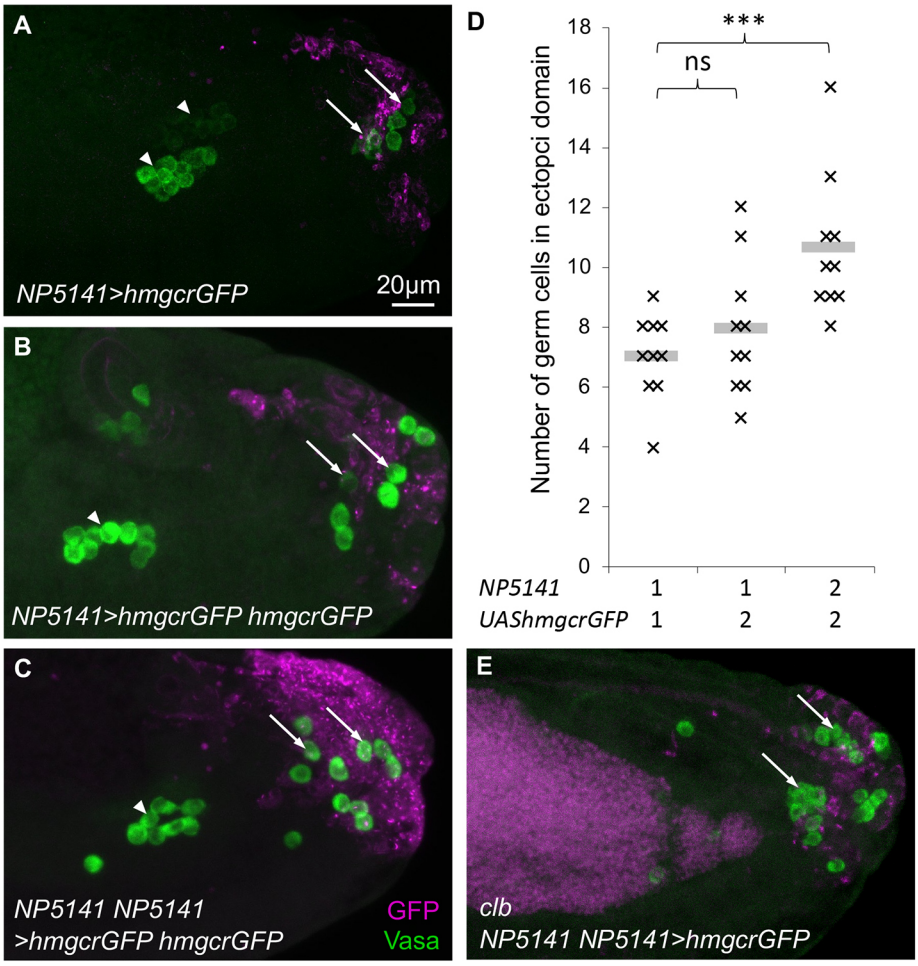


**Fig. 4. The range of the Hmgcr-mediated signal is concentration dependent.** (A–C,E) Maximum intensity projections of lateral views of representative stage 14 embryos of the genotypes: (A) *NP5141Gal4/+;UASHmgcrGFP/+*, (B) *NP5141Gal4/+;UASHmgcrGFP/ UASHmgcrGFP*, (C) *NP5141Gal4/NP5141Gal4; UASHmgcrGFP/ UASHmgcrGFP* and (E) *NP5141Gal4/NP5141Gal4; clb$^{11.54}$ UASHmgcrGFP/ clb$^{11.54}$* fluorescently stained with antibodies against Vasa to label germ cells (green) and GFP to visualise the ectopic domain (magenta). In E, nearly all of the germ cells (25 out of the 27) are located in the ectopic domain. Arrows indicate germ cells in the ectopic domain. Arrowheads indicate the embryonic gonads. (D) Graph showing number of germ cells in the ectopic domain in stage 13–14 embryos with different numbers of copies of the UAS and Gal4 transgenes (the same as the genotypes depicted in A–C). Mean values are indicated by a grey bar. ***$P$<0.001; ns, not significant (two-tailed Student's $t$-test).

Journal of Cell Science (2019) 132, jcs232637. doi:10.1242/jcs.232637

mutant embryos expressing ectopic GFP and remained at that same distance in stage 11 and 12 embryos (data not shown). Therefore, with higher levels of Hmgcr expression, the range of the Hmgcr-mediated signal is increased. Taken together, we conclude that the range of attraction of the Hmgcr-mediated signal is dependent on the level of Hmgcr expression and these data support that it acts at a long range.

### Live imaging of ectopic germ cell attraction supports the long-range nature of the signal

So far, we have estimated the range of the *Hmgcr*-mediated signal by analysing germ cells in fixed embryos. To see whether we could observe germ cells being ectopically attracted over such distances in living embryos, we used light-sheet microscopy and a *nanos>moeGFP* construct to visualise the germ cells (Sano et al., 2005).

In a control embryo, in which the amnioserosa was labelled with GFP using *Krüppel-Gal4* and *UAS GFP* constructs, to visualise the germ band movements of the embryo, the germ cells moved from the posterior midgut pocket to the gonad over a period of ∼6 h. The path of migration and the lack of noticeable germ cell death indicates that the embryos were not adversely affected under the imaging conditions used (Fig. 5A).

In an experimental embryo in which the ectopic domain expressed untagged *Hmgcr* to avoid interference with the germ cell labelling, we observed germ cells migrating to the ectopic domain. We tracked the majority of germ cells and colour coded them according to whether they migrated to the gonad (Fig. 5B, blue/cyan tracks), to the ectopic domain (Fig. 5B, pink/purple tracks) or that remained at the midline (Fig. 5B, yellow tracks). We saw that germ cells entered the ectopic domain from late stage 10 and continued to enter until late stage 12 (Fig. 5B,C). Once associated with the gonad at stage 13, germ cells remained there and did not exit and migrate to the ectopic domain. These observations are in agreement with those from the fixed embryo analysis. Once in the ectopic domain, germ cells remained there and stopped migration, indicating that high levels of *Hmgcr* even in non-SGP somatic cells are sufficient to stop the migratory programme of the germ cells (Fig. 5B).

We then focused on the portions of migratory movements of germ cells entering the ectopic domain in which the germ cells broke away from the normal migratory path. We measured the distance

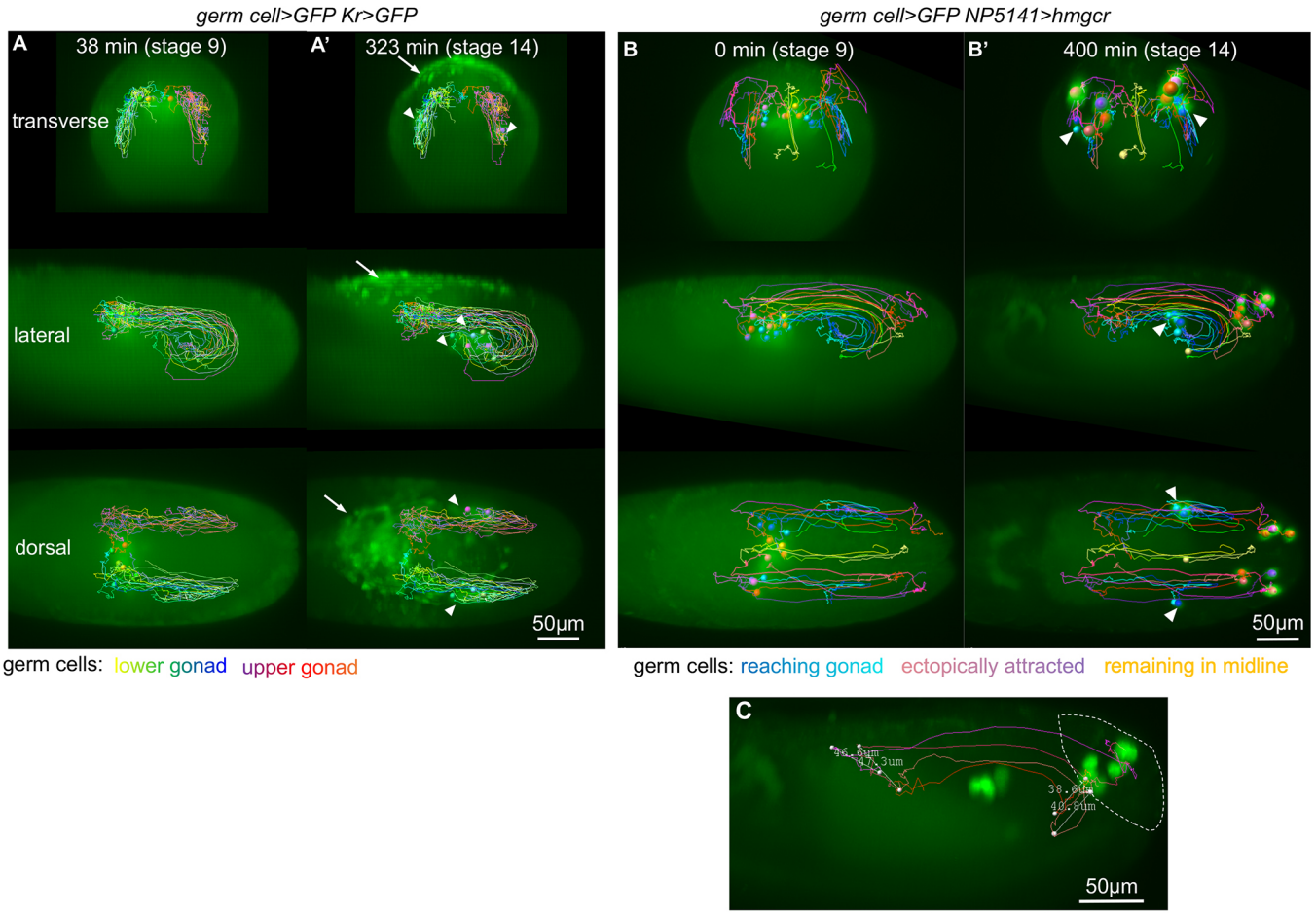


**Fig. 5. Live imaging of ectopic Hmgcr attracting germ cells.** (A,B) Transverse (upper), lateral (middle) and dorsal (lower) views from 3D reconstructions of movies of embryos with the genotypes: (A) *nos>moeGFP;;PrDr/TM3KrGal4UASGFP* (see Movies 1,2), (B) *nos>moeGFP;NP5141Gal4/+;UASHmgcr/+* (see Movies 3,4). Germ cells were tracked and coloured according to their final position. Arrows indicate amnioserosa labelling in the control embryo from the *KrGal4UASGFP* transgenes. Arrowheads indicate the embryonic gonads. (C) Lateral view taken from embryo in B showing germ cell tracks for four germ cells that ended up in the ectopic domain; two entered it at stage 11 and two entered at late stage 12 (left and right measurements, respectively). Linear distances between the germ cell position when it first began moving into the ectopic domain and when it stopped migrating as it entered the ectopic domain are indicated. Estimated boundary of ectopic domain at stage 13 (when the germ band has fully retracted) is indicated by dashed lines.

Journal of Cell Science (2019) 132, jcs232637. doi:10.1242/jcs.232637

over which this abnormal migration took place (Fig. 5C). At stage 11, we observed two germ cells each migrating for ∼47 µm to enter the ectopic domain and at late stage 12 we observed two germ cells migrating 39 µm and 41 µm to enter the ectopic domain (Fig. 5C). These distances are in strong agreement with our estimates of a range of 51 µm from fixed embryos (Fig. 3D) and support the notion that *Hmgcr* is mediating a long-range signal.

### Germ cells are within range of the *Hmgcr*-mediated signal throughout their migratory journey

To see how our estimate for the range of the *Hmgcr*-mediated signal compares to the distance of germ cells to *Hmgcr*-expressing SGPs in wild-type embryos, we measured such distances in stage 10 and 11 embryos (Fig. 6A–C). We found that germ cells were located between 5 and 58 µm from their closest SGP at stage 10 and ranged from 0 to 30 µm at stage 11. Therefore, for stages 10 and 11, 98% and 100% of germ cells respectively would be within our estimate of 51 µm for the range of the *Hmgcr*-mediated signal. We conclude that germ cells are potentially under the influence of the *Hmgcr*-mediated signal for their entire migratory journey.

### *Hmgcr* and *wun* operate simultaneously

We next wanted to know which of the two pathways, Hmgcr or Wunen, is dominant. To do this we gave germ cells conflicting guidance cues by simultaneously attracting them to the ectopic domain using *Hmgcr* expression and repelling them by co-expressing *wun*. When *wun* is expressed using the *NP5141* Gal4 driver there is no effect on overall germ cell migration (Mukherjee et al., 2013; Fig. 7A–D). When *wun* and *Hmgcr* are co-expressed, germ cells are still attracted towards the ectopic domain to a similar degree to when *Hmgcr* was expressed alone (Fig. 7E–H). However, despite some germ cells arriving at the ectopic domain as early as

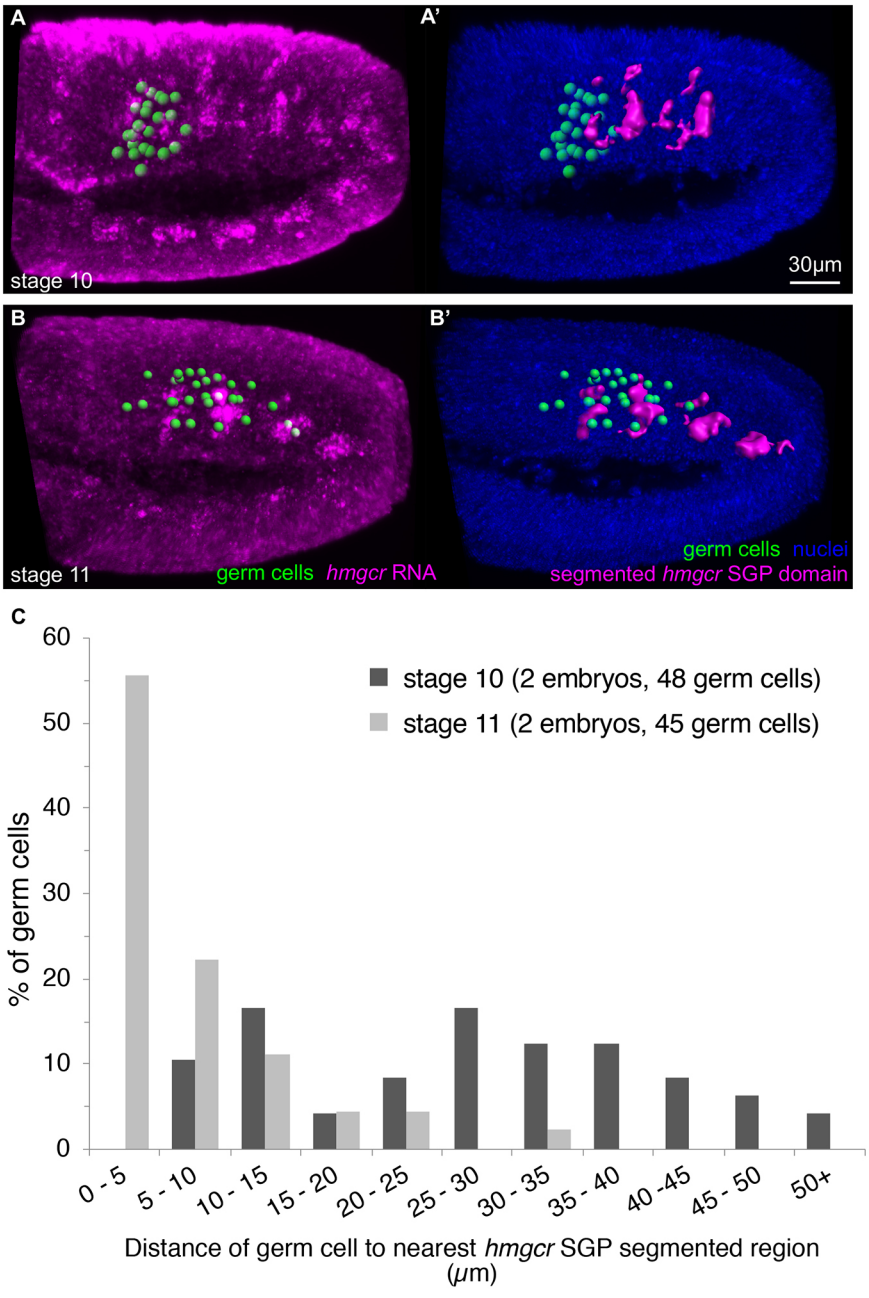


**Fig. 6. The majority of germ cells are within the range of the *Hmgcr*-mediated signal.** (A,B) Lateral views of 3D reconstructions of stage 10 (A) and stage 11 (B) wild-type embryos that have been fluorescently stained with antibody against Vasa to label germ cells, an RNA probe for *Hmgcr* (magenta in A and B) and DAPI, to label nuclei (blue). Germ cells positions were manually scored (green spheres) and *Hmgcr*-expressing SGP clusters were computationally segmented (magenta in A′ and B′). Other *Hmgcr*-expressing domains were not segmented. (C) Graph showing frequency of germ cells located at distances indicated from their nearest *Hmgcr*-expressing SGP cluster at stages 10 and 11 in wild-type embryos.

Journal of Cell Science (2019) 132, jcs232637. doi:10.1242/jcs.232637

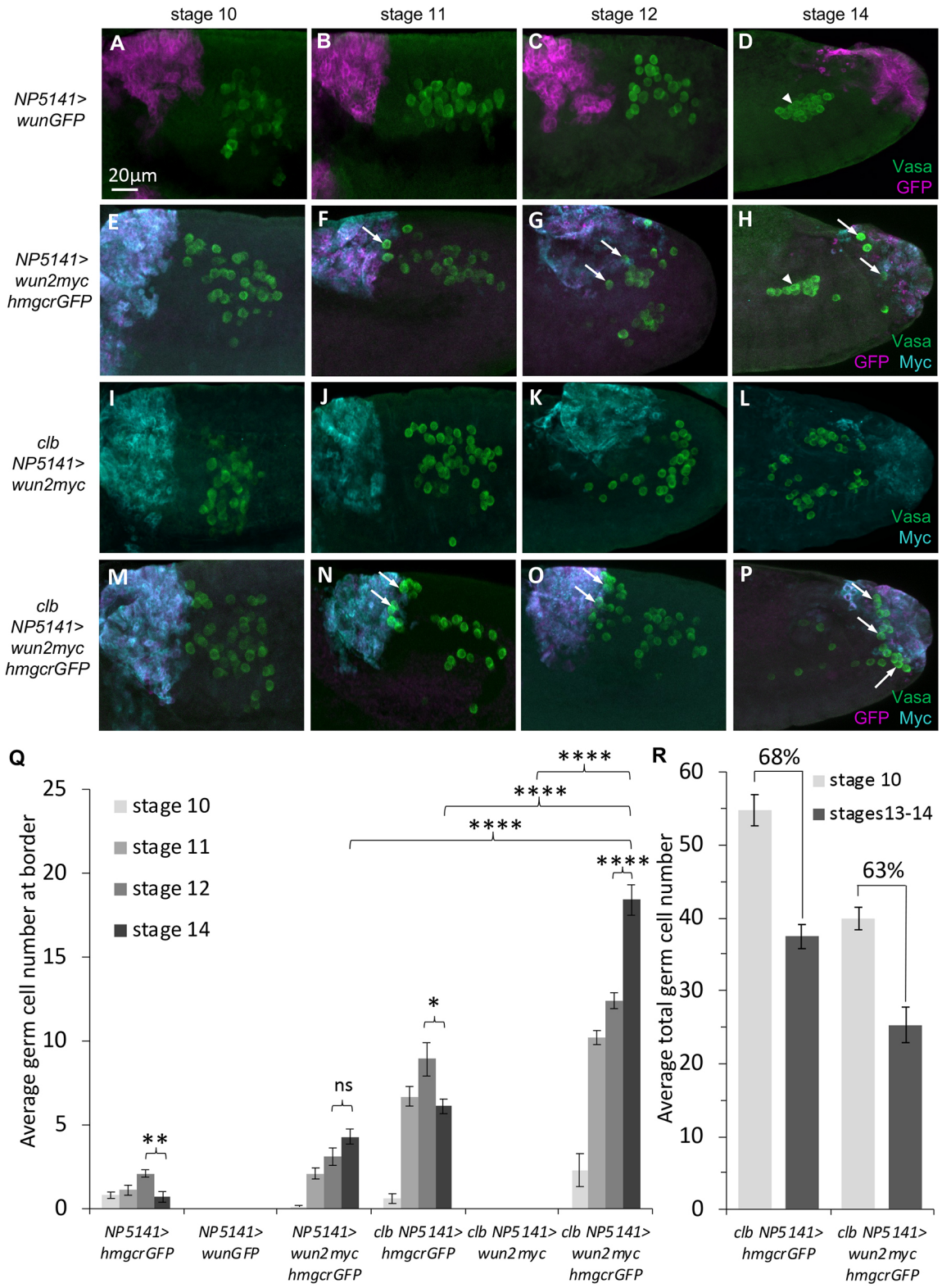


**Fig. 7. The Hmgcr and Wunen pathways can operate simultaneously.** (A–P) Maximum intensity projections of lateral views of representative stage 10–14 embryos, of genotypes: (A–D) *NP5141Gal4/UASwunGFP*, (E–H) *NP5141Gal4/UASwun2myc; UASHmgcrGFP/+*, (I–L) *NP5141Gal4/UASwun2myc;clb$^{11.54}$/clb$^{11.54}$* and (M–P) *NP5141Gal4/UASwun2myc;clb$^{11.54}$UASHmgcrGFP/clb$^{11.54}$* fluorescently stained with antibodies against Vasa to label germ cells (green), and GFP and Myc to visualise ectopic expression (magenta and cyan, respectively). Arrowheads indicate the position of the embryonic gonads, and arrows indicate germ cells that are at the ectopic domain border. (Q) Graph showing the mean±s.e.m. number of germ cells at the ectopic domain border in stage 10–14 embryos. *n*=10 embryos scored per genotype. *P*-values calculated by Student's *t*-test (two tailed). Images for *NP5141>HmgcrGFP* and *clb NP5141>HmgcrGFP* embryos are given in Fig. 1F–I and 1N–Q, respectively. *n*=10 embryos scored per genotype. **P*<0.05; ***P*<0.01; *****P*<0.0001; ns, not significant (two-tailed Student's *t*-test). (R) Graph showing the mean±s.e.m. total germ cell number per embryo between stages 10 and 13–14 embryos. In both genotypes, germ cell numbers decrease but the percentage of germ cells surviving is similar, indicating that *wun* co-expression is not causing extensive germ cell death.

Journal of Cell Science (2019) 132, jcs232637. doi:10.1242/jcs.232637

stage 11 (Fig. 7F), germ cells are not subsequently found within the ectopic domain but instead remain at its boundary (Fig. 7G,H).

This positioning of the germ cells could result from attraction to the ectopic domain by *Hmgcr* and then *wunen* activity either repelling germ cells from entering the domain or killing those germ cells that do enter, as happens for example when Wunens are ectopically expressed in the mesoderm (Starz-Gaiano et al., 2001). To distinguish between these two hypotheses, we tested what would happen if larger numbers of germ cells were to be attracted to the ectopic domain. We performed the same experiment in a *clb* mutant background in which competition for attraction by the SGPs is eliminated. In this scenario, the number of germ cells attracted to the ectopic domain was indeed increased and significantly more germ cells accumulated at the ectopic domain boundary (Fig. 7M–Q).

Despite the large number of germ cells being attracted, we did not observe germ cells or remnants of dying germ cells inside the ectopic domain, making it unlikely that germ cells were entering the ectopic domain and dying. This interpretation is supported by two further pieces of evidence. The first is the change in the number of germ cells at the ectopic domain border between stages 12 and 14. In the case of *Hmgcr* expression in both wild-type and *clb* mutant backgrounds, this number decreases as germ cells move past the border and enter the domain. When *wun* is co-expressed, however, this number increases as more germ cells arrive and those already present fail to move past the border (Fig. 7Q). If germ cells were dying then we would predict that this number would fall as germ cells enter the domain and then die. The second is the overall germ cell survival rate between stage 10 and stages 13–14, which is similar in embryos ectopically expressing *Hmgcr* in a *clb* mutant background compared to those ectopically expressing both *wun* and *Hmgcr* in a *clb* mutant background (Fig. 7R). This suggests that co-expression of *wun* is not causing extensive germ cell death.

These data show that Wunens can repel germ cells and prevent them from entering an *Hmgcr*-expressing ectopic domain. Taken together, we conclude that neither the *wun* nor the *Hmgcr* pathway is dominant and germ cells position themselves using the information provided by both pathways simultaneously.

### *hh* is not required downstream of *Hmgcr* for germ cell attraction

We wanted to test whether *hh* is required downstream of *Hmgcr* for the attraction of germ cells. We therefore asked whether germ cells could be attracted to ectopic *Hmgcr* in an *hh*-null background. If *hh* is the attractant downstream of *Hmgcr*, we would predict that germ cells would not be attracted to *Hmgcr* in a *hh* background. On the other hand, if *hh* is not the downstream attractant, we would predict that germ cells would still be attracted to ectopic *Hmgcr* in a *hh* mutant.

We used the null allele, $hh^{AC}$, which, when homozygous, causes embryos to have cuticles with a characteristic strong *hh* phenotype consisting of a continuous lawn of denticles identical to that published in Lee et al. (1992) (Fig. S6A,B). $hh^{AC}$ embryos have very severe patterning defects that are evident from stage 13, which causes germ cells to scatter over the poorly patterned posterior of the embryo. Therefore, we examined earlier $hh^{AC}$ embryos, at stage 12, when germ cells are mostly on track and none have mismigrated into a control ectopic domain that expresses just GFP (Fig. 8A,B). We founnd that ectopic expression of *HmgcrGFP* can attract germ cells in *hh* homozygous mutant embryos similar to in sibling heterozygous controls (Fig. 8C–E). We conclude that zygotic *hh* is not required downstream of *Hmgcr* for attracting germ cells.

One caveat is a potential for maternally provided *hh* message to be a source of Hh that acts downstream of *Hmgcr*. Although maternal *hh* message was not previously detected by northern blot analysis (Lee et al., 1992), we checked for potential perdurance of maternal *hh* mRNA in the ectopic domain by *in situ* hybridisation. We do not see *hh* mRNA at stage 10 in $hh^{AC}$ mutant embryos (Fig. S6E,F), therefore we find no evidence of a role for maternally provided *hh* downstream of *Hmgcr*.

To test whether *hh* could be acting as a germ cell attractant independently of *Hmgcr*, we also tested whether ectopic *hh* expression from the *NP5141* Gal4 driver was sufficient to attract germ cells. We found no mis-migrated germ cells in this domain under these conditions (Fig. 8E) despite the *UAS hh* construct being able to induce patterning defects identical to that seen in Fietz et al. (1995) when expressed using a *patched* Gal4 driver (Fig. S6C,D). Taken together, these data support the conclusion that *hh* is not the germ cell attractant downstream of *Hmgcr*.

## DISCUSSION

Here, we have examined the range of influence of a signal downstream of *Hmgcr* that attracts germ cells in *Drosophila* embryos. We have found that this signal can act at distances of at least 51 µm and is dependent on the levels of *Hmgcr* overexpression. This distance is greater than the distance of virtually all of the germ cells from the target SGPs at stages 10 and 11 and therefore, distance-wise at least, should be sufficient to attract germ cells to the gonad. Furthermore, the signal can operate at the same time as a second pathway, namely that mediated by the Wunens. This is most strikingly demonstrated by finding that the simultaneous overexpression of both components in the same ectopic domain produces a phenotype different from that seen upon overexpression of either component alone, in that we see both simultaneous attraction and repulsion as the germ cells line up at the edge of the expression zone. Finally, we provide evidence that the extracellular signalling molecule Hh is not the chemoattractant downstream of *Hmgcr*.

Our 51 µm estimate of the range of the *Hmgcr*-mediated signal represents approximately six germ cell diameters (*Drosophila* germ cells being 8–9 µm in diameter, Fig. S5) or nine mesodermal cell diameters (*Drosophila* stage 12 mesodermal cells being ∼5–7 µm in diameter, Fig. S5), which would make it a long-range signal. This range is broadly in line with other long-distance signalling molecules in *Drosophila* and other species. For instance, in *Drosophila* imaginal wing discs the TGF-β family member Dpp acts at long range, influencing cells up to 20 cell diameters away (Nellen et al., 1996). In *Xenopus* embryos, TGF-β ligands can be detected 7–10 cell diameters away from their source (McDowell et al., 2001; Williams et al., 2004), while in zebrafish embryos, cells can respond to endogenous TGF-β (nodal) signalling at distances up to 200 µm (Harvey and Smith, 2009). The mean total length of the tracks of successfully migrating germ cells in our live imaging movies (from early stage 10 to stage 13) is 381 µm (s.e.m. 18.4 µm) (Fig. 5). Although this is much longer than our estimate of the range of the *Hmgcr*-mediated signal, much germ cell movement is non-cell autonomous and comes from the bulk embryonic movements of germband retraction.

Wnt ligands on the other hand can act at either short or long range. Wingless acts as a short-range inducer in *Drosophila* embryos, being secreted by stripes of ectodermal cells and being received only by their neighbours (van den Heuvel et al., 1989). In mouse organoids, Wnt3 also acts at short range being visualised only 1–2 cells away from synthesising cells (Farin et al., 2016). On

Journal of Cell Science (2019) 132, jcs232637. doi:10.1242/jcs.232637

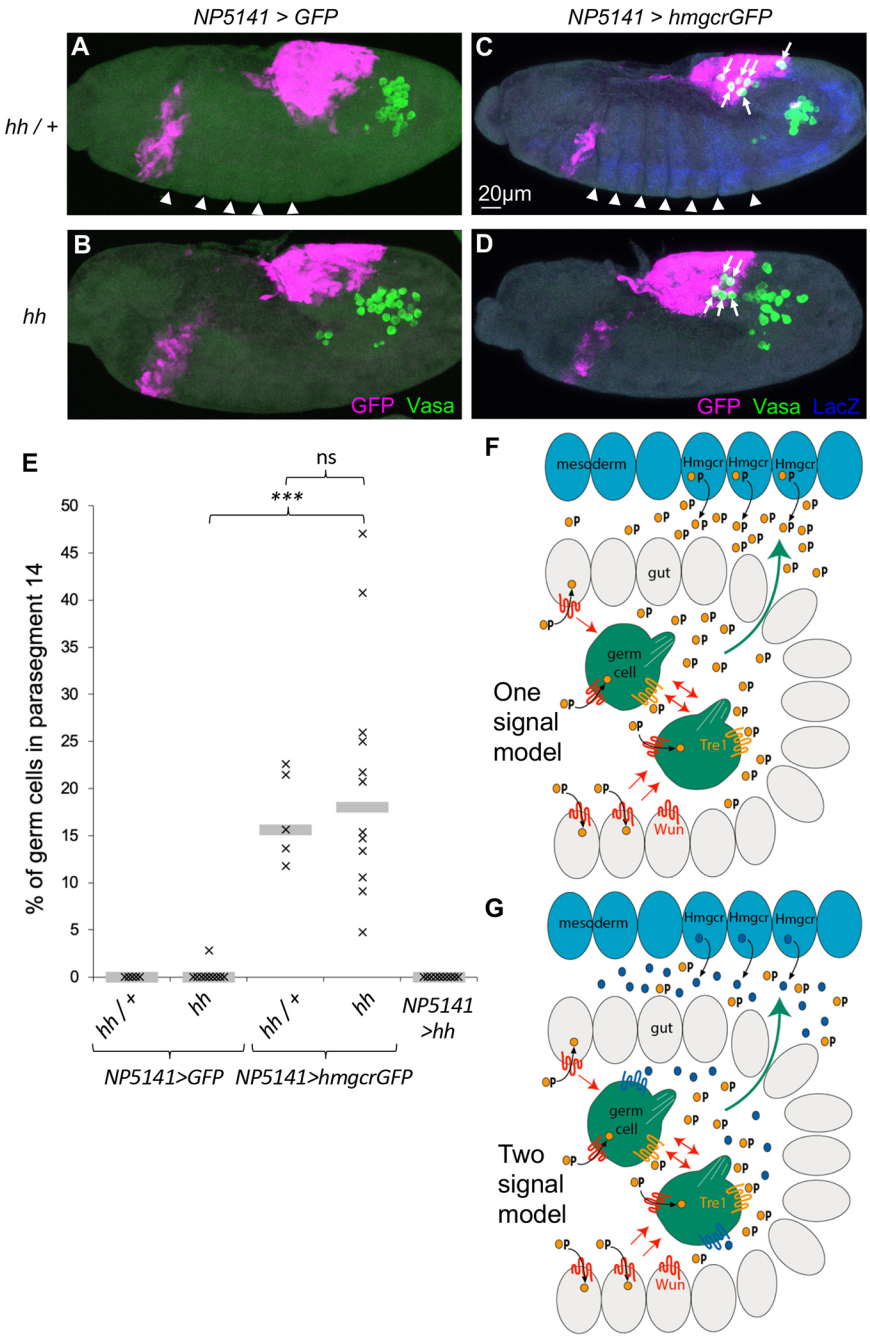


**Fig. 8. Hh is not downstream of *Hmgcr* in the germ cell attraction pathway, and models for signals downstream of Wunen and Hmgcr.** (A–D) Maximum intensity projections of lateral views of representative stage 12 embryos of genotypes: (A) *NP5141Gal4/UASGFP;hh$^{AC}$/+*, (B) *NP5141Gal4/UASGFP;hh$^{AC}$/hh$^{AC}$*, (C) *NP5141Gal4/NP5141Gal4; UASHmgcrGFP hh$^{AC}$/TM3 ftz>lacZ* and (D) *NP5141Gal4/NP5141Gal4; UASHmgcrGFP hh$^{AC}$/UASHmgcrGFP hh$^{AC}$* fluorescently stained with antibodies against Vasa to label germ cells (green) and GFP to visualise the ectopic domain (magenta). Heterozygous and homozygous *hh$^{AC}$* embryos were distinguished by staining with an antibody against LacZ (blue, C and D) and by loss of parasegmental furrows in the germ band (arrowheads in A and C). Germ cells located in parasegment 14 (the posterior *NP5141*-expressing domain) are marked with arrows. (E) Graph showing number of germ cells located in parasegment 14 as a percentage of the total for individual embryos of the genotypes depicted in A–D as well as upon *hh* overexpression. Median values are indicated by a grey bar. ***$P$<0.001; ns, not significant (Mann–Whitney $U$-test). (F,G) Schematic of lateral views of a stage 9 embryo with germ cells inside the posterior midgut being attracted (green arrow) towards Hmgcr-expressing mesodermal cells (blue cells) and being repelled from regions of somatic Wun expression and each other due to germ cell Wun expression (red arrows). (F) In a one-signal model, Hmgcr expression results in release of a phosphorylated chemoattractant (orange circles), which is detected on germ cells via Tre1 and dephosphorylated by Wunens, acting as a sink. (G) In a two-signal model, Hmgcr expression results in release of a chemoattractant (blue circles), unrelated to Wun, which is detected on germ cells via a receptor other than Tre1 (blue receptor). Localised Wunen expression (on germ cells and some somatic cells) acts as a sink for a second chemoattractant (orange circles) via dephosphorylation. This second chemoattractant is detected on germ cells by Tre1 (orange receptor).

the other hand, Wingless in *Drosophila* imaginal wing discs acts at long range, influencing cells 20 or more cell diameters away (Zecca et al., 1996), and EGL-20 in *C. elegans* can be seen in a gradient up to 50 µm from its source (Coudreuse et al., 2006).

In these examples, the ligands are providing positional information to static cells by inducing concentration-dependent transcriptional responses. In the case of the Hmgcr and Wunen, however, the responding germ cells are motile, and a transcriptional response seems unlikely given the speed and the need for signal directionally not just strength. Ligands acting in a similar fashion include chemokines such as stromal cell-derived factor 1 (SDF1; also known as CXCL12), which acts as a long-range attractant for several cell types. SDF-1a-expressing cells transplanted into zebrafish embryos can attract germ cells over distances of at least 250 µm (Blaser et al., 2005), and SDF-1-soaked beads can attract interneurons in mouse brain slice cultures over similar distances (Li et al., 2008).

We have estimated the distance over which *Hmgcr* is potentially able to operate via overexpression studies and shown that the range is influenced by the degree of overexpression. To ascertain the relevance of our distance estimations to the wild-type situation, we have compared the number of cells expressing *Hmgcr* ectopically to those normally expressing *Hmgcr*. We estimate there are just over 1000 *HmgcrGFP* ectopically expressing cells in parasegment 14 at stage 10 when driven by *NP5141* Gal4 (Fig. S3A). At stages 9–10, *Hmgcr* is expressed broadly in the mesoderm (Van Doren et al., 1998). We estimate there are ∼250 *Hmgcr*-expressing mesodermal cells at stage 10 that lie dorsally to the germ cells, and to which the germ cells will migrate (Fig. S3B). By stage 12, *Hmgcr* is highly expressed in the SGPs (Van Doren et al., 1998) of which there are

Journal of Cell Science (2019) 132, jcs232637. doi:10.1242/jcs.232637

only 25–35 cells in total per gonad (Sonnenblick, 1941). Therefore, the number of cells ectopically versus endogenously expressing *Hmgcr* is comparable, at least at early stages.

We have examined whether the *wunen* and *Hmgcr* pathways act simultaneously rather than consecutively. We found that the pathways can act simultaneously when *wunen* and *Hmgcr* are overexpressed (Fig. 6M–P). We believe that the behaviour of the germ cells in these ectopic expression experiments is relevant to the wild-type scenario because *wun2* and *Hmgcr* are normally expressed at the same time, although in different parts of the embryo, throughout the period when germ cells are migrating (Starz-Gaiano et al., 2001; Van Doren et al., 1998 and Fig. S3B,D).

There are two possible models of the interactions between Hmgcr and Wunen (Fig. 8F,G). The prevailing view is a two-signal model (Fig. 8G; Barton et al., 2016). One chemoattractant results from Hmgcr expression in the mesoderm and is perceived by germ cells via an unidentified receptor. The second chemoattractant is perceived by germ cells using the Tre1 GPCR (LeBlanc and Lehmann, 2017). It is also a substrate for the Wunens and is dephosphorylated and thereby destroyed by Wunen-expressing cells, including the germ cells, which collectively act as a chemoattractant sink. In this model, the spatial information provided by Hmgcr and Wunens is integrated at the level of the germ cells, which use the information provided by both chemoattractants.

In a one-signal model, Hmgcr expression would result in secretion of a chemoattractant from the mesoderm that is also the substrate for the Wunens and is detected on germ cells by the Tre1 GPCR (Fig. 8F). In this model, the spatial information provided by Hmgcr and Wunens is integrated at the level of the chemoattractant gradient, which depends on the combined actions of both of these enzymes.

Both models have precedents from other extracellular gradients both in *Drosophila* and other organisms. The one-signal model (Fig. 8F) resembles classical source–sink models for both chemoattractant and morphogen gradients (Cai and Montell, 2014). The use of simultaneous attraction and repulsion, as per the two-signal model (Fig. 8G), is seen in *Drosophila* axonal pathfinding where commissural axons are attracted and repelled by the ligands Netrin and Slit, respectively (Dickson and Gilestro, 2006). The migration of vertebrate trunk neural crest cells is controlled by both positive and negative regulators including ligand–receptor pairs such as ephrin–Eph, and Sdf1–Cxcr4 (Shellard and Mayor, 2016).

Our data do not definitively discriminate between these two models. In support of the one-signal model (Fig. 8F) we note, firstly, that the signals downstream of both Wunens and Hmgcr operate over similar long ranges, which means they are potentially the same molecule. Secondly, zygotic loss of function mutants of *wun* and *clb* both exhibit similar very strong mis-migration phenotypes with few germ cells reaching the gonad in either mutant alone (Van Doren et al., 1998; Zhang et al., 1997) similar to what is seen in the double mutant (Fig. 2E). If each pathway influenced their own independent signal, then one might expect that removal of either pathway alone would result in partial germ cell mis-migration (with only some germ cells mis-migrating) as the other would still be active and also acting over a long range.

However, some of our data are difficult to reconcile with a single signal. We would have expected that if ectopic Wunens are degrading a signal generated by ectopic Hmgcr, co-expression would decrease the range of the signal and delay the time at which cells mis-migrate to the border. However, we see almost as many germ cells at the ectopic domain border (Fig. 7P) when both HmgcrGFP and Wun are expressed in the ectopic domain in a *clb* mutant background, as we see germ cells inside the ectopic domain when just HmgcrGFP is expressed there in a *clb* mutant background (Fig. 1Q). Germ cells also reach the border at similar stages in these two conditions (compare *clb NP5141>HmgcrGFP* with *clb NP5141>wun2myc HmgcrGFP* in Fig. 7Q). Therefore, either any decrease in range is minimal or there are two signals. The alignment of germ cells at the ectopic domain border is surprisingly precise given that the Wunen-dependent signal can be contact independent and long range (Mukherjee et al., 2013). This opens up the possibility that there are several *in vivo* substrates of the Wunens, like there are *in vitro* (Renault et al., 2004), some of which could act at much shorter range.

The ultimate confirmation of which model is correct will require identification of the chemoattractant(s). It is interesting to note that germ cell migration in other species such as chicken and zebrafish seems to require only a single chemoattractant (SDF-1) in spite of the much longer migratory journeys, both in terms of distance and time, in these species (Barton et al., 2016). It is clear that *Drosophila* germ cells cannot be responding to SDF-1 as no SDF-1 homologue exists in flies. What is less clear is whether the signals downstream of *wunens* and *Hmgcr* exist in vertebrates, perhaps playing a more subtle role. Tantalising evidence from zebrafish suggests this might be the case, with simultaneous knockdown of all the Wunen homologues causing some germ cells to mis-migrate (Paksa et al., 2016). Therefore, the cues that regulate *Drosophila* germ cell migration might actually be more conserved than we first thought. In addition, Hmgcr overexpression in stomal cells acts in a paracrine fashion to promote prostate cancer cell growth (Ashida et al., 2017) suggesting that Hmgcr-mediated signals are also relevant in humans to tumour progression and metastasis.

## MATERIALS AND METHODS

### Fly stocks

The following *Drosophila* lines were described previously: $Df(2R)wun^{GL}$, a deficiency removing *wun* and *wun2* (Zhang et al., 1996); $clb^{11.54}$, a loss of function allele of *Hmgcr* (Van Doren et al., 1998); $hh^{AC}$, an amorphic allele resulting from a 8.6 kb deletion removing the promoter and part of the coding region (Lee et al., 1992); *UAS wunGFP* (Burnett and Howard, 2003); *UAS wun2myc* (Starz-Gaiano et al., 2001) [the *wunGFP* and *wun2myc* constructs behave indistinguishably – both can rescue the tracheal phenotypes caused by *wun* loss of function and both cause identical amounts of germ cell death when ubiquitously embryonically overexpressed (Ile et al., 2012)]; *UAS lazGFP* (Garcia-Murillas et al., 2006), expression of which does not affect germ cells (Mukherjee et al., 2013); *UAS Hmgcr* (Van Doren et al., 1998); *UAS CD2* (Dunin-Borkowski and Brown, 1995); $Hmgcr^{EY04833}$, a UAS-containing insertion 5′ of the *Hmgcr* gene (stock 16619, Bloomington Stock Center); *p(GawB)NP5141*, a Gal4-containing insertion 5′ of the gene *ken* (*Drosophila* Genetic Resource Center); *y M{vas-int.Dm}ZH-2A w; PBac{y*$^{+}$*-attP-3B}VK00033* used as a landing site for the *UASHmgcrGFP* transgene. *nanos>moeGFP* was used to label the germ cells for live imaging (Sano et al., 2005). The following labelled balancer chromosomes were used: TM3 *P{w[+mC]=GAL4-Kr.C}DC2, P{w[+mC]=UAS-GFP.S65T}DC10*, *Sb1* and TM3 *P{ftz-lacZ.ry+}TM3, Sb1 ry**.

### Immunohistochemistry and imaging

Embryos were laid at room temperature, dechorionated in 50% bleach for 3 min, fixed for 20 min in 4% formaldehyde (37% for *in situ* hybridisation) in PBS–heptane, devitellinised using heptane–methanol, and stained using standard protocols. Primary antibodies were as follows: polyclonal rabbit anti-Vasa (courtesy of Ruth Lehmann, Skirball Institute of Biomolecular Medicine, New York, USA, 1:10,000), rabbit anti-LacZ (MP Biomedicals

559761, lot 06680, 1:10,000), chicken anti-GFP (Abcam ab13970, lot GR89472-6, 1:1000), rabbit anti-MYC (Abcam ab9106, lot GR41743-1, 1:1000), mouse α-spectrin (DSHB 3A9, 1:10) and mouse anti-CD2 (Bio-Rad MCA154GA, lot 0515, 1:2000). Secondary antibodies conjugated to Alexa Fluor 488 or 648 (Invitrogen) and Cy3 (Jackson ImmunoResearch) were used at 1:500.

To visualise *Hmgcr* or *wun2* expression, full-length *Hmgcr* or *wun2* cDNA clones in pNB40 and pBSK vectors, respectively, were linearised and used to make a digoxygenin-labelled RNA probe by *in vitro* transcription with T7 RNA polymerase, and hybridisation and fluorescent detection was carried out as described previously (Lécuyer et al., 2008). To visualise *hh* expression, an 800 bp fragment of *hh* coding sequence was amplified by PCR from cDNA using the primers 5′-GATCGTCTTGCCGATGGTCT-3′ and 5′-CACAAACGTGAGCTTCTGGC-3′ and cloned into pGEM T-easy vector (Promega). The vector was linearised and used to make a digoxygenin-labelled RNA probe by *in vitro* transcription, and hybridisation and colourimetric detection was carried out as described previously (Lehmann and Tautz, 1994).

Fluorescently stained embryos were either mounted in aquamount (Polysciences) or dehydrated in methanol and mounted in benzylbenzoate–benzyl alcohol (2:1). Images were acquired using an LSM 880 confocal microscope with a 20× NA 0.5 air or 40× NA 1.3 oil objective and Zeiss Zen2 acquisition software. Live imaging was performed on a Zeiss Z1 light-sheet microscope. Embryos were aged until approximately stage 9, dechorionated, transferred into cooled, but still liquid, 1% low-melt agarose dissolved in distilled water, and drawn into a glass capillary. Once the agarose had set, the capillary tube was transferred to the light-sheet microscope and embryos imaged with a 20× NA 0.5 air objective using the 488 nm laser until the end of embryogenesis. Such embryos were able to hatch into larvae, indicating that the conditions used did not noticeably impair development. Germ cells were tracked using Imaris software (Bitplane).

### Image analysis

3D reconstructions, segmentations and distance measurements were made with Imaris software (Bitplane). For germ cell distance measurements, late stage 10 embryos were chosen in which the germ cells had exited the posterior midgut. Germ cell positions were detected automatically (using the spots tool) and manually edited for accuracy. The ectopic domain was segmented using the surfaces tool, and the distance of the edge of each spot (using the Imaris minimum intensity statistic) to the nearest ectopic domain surface was measured using the MeasurementPro extension. Germ cells that were ‘stuck’ in the midgut or hindgut were identified by both being in a tight round or elongated cluster and inside a tubular structure visible as background fluorescence by increasing the channel brightness. For the scoring of germ cells inside the ectopic domain in Fig. 2G, the ectopic domain was labelled using GFP or HmgcrGFP, with the exception of *wun wun2 clb* mutant embryos where instead the number of germ cells within 50 µm of the embryo posterior (this being the mean length of the ectopic domain in *NP5141>GFP* embryos) was used.

The volumes of the *NP5141>HmgcrGFP* domain in stage 14 embryos was determined using the segmentation function of Imaris (Bitplane). The number of cells in the *NP5141* domain and in the wild-type *Hmgcr*-expressing domain were scored manually in ImageJ using the cell counter plugin. The diameters of germ cells and mesodermal cells were measured in ImageJ.

Germ cell survival rates were calculated as the average total number of germ cells in stage 13–14 embryos divided by the average total number of germ cells in stage 10 embryos (when the germ cells leave the tight cluster in the posterior midgut and become easily scorable).

### Generation of *UASHmgcrGFP* flies

The *Hmgcr* coding sequence was amplified from cDNA clone in pNB40 using the primers 5′-CACCATGAGGACGTTTGTTTCGC-3′ and 5′-GCTGATGGGCTGCAGCTGG-3′ and cloned into the pENTR/*D-TOPO* vector (Invitrogen). The sequence was verified and moved into the destination vector pUAST-*attB*-WG (a gift from Saverio Brogna, School of Biosciences, University of Birmingham, UK, producing C-terminal GFP fusions) with the use of the Gateway reaction. This resulting expression vector pUAST-*attB-Hmgcr*-WG was microinjected into embryos containing phiC31 integrase and an *attP* site on the third chromosome.

#### Acknowledgements

We thank Tom Starkey for recombinant fly stocks, the University of Nottingham School of Life Sciences Microscope facility for training on and access to the Zeiss 880 confocal microscope, and Malcolm Bennett and Antony Bishopp (School of Biosciences, University of Nottingham) for use of the Zeiss Z1 light-sheet microscope (funded through BBSRC award BB/M012212/1). We thank Christian Feldhaus (Max Planck Institute for Developmental Biology) for assistance with distance measurements in Imaris and Markus Owen, Andrew Johnson and Fred Sablitzky (University of Nottingham) for manuscript comments. We acknowledge the Flybase consortium for gene information and the Bloomington Stock Center at Indiana University for stocks. We thank the Saverio Brogna laboratory for reagents.

#### Competing interests

The authors declare no competing or financial interests.

#### Author contributions

Conceptualization: K.K., A.D.R.; Methodology: K.K., A.D.R.; Formal analysis: K.K., A.D.R.; Investigation: K.K., A.M., A.D.R.; Writing - original draft: A.D.R.; Writing - review & editing: A.M., A.D.R.; Supervision: A.D.R.; Project administration: A.D.R.; Funding acquisition: A.D.R.

#### Funding

K.K. was supported by a University of Nottingham studentship.

#### Supplementary information

Supplementary information available online at
http://jcs.biologists.org/lookup/doi/10.1242/jcs.232637.supplemental

#### References

**Ashida, S., Kawada, C. and Inoue, K.** (2017). Stromal regulation of prostate cancer cell growth by mevalonate pathway enzymes HMGCS1 and HMGCR. *Oncol. Lett.* **14**, 6533-6542. doi:10.3892/ol.2017.7025

**Barton, L. J., LeBlanc, M. G. and Lehmann, R.** (2016). Finding their way: themes in germ cell migration. *Curr. Opin. Cell Biol.* **42**, 128-137. doi:10.1016/j.ceb.2016.07.007

**Bellés, X., Martín, D. and Piulachs, M.-D.** (2005). The mevalonate pathway and the synthesis of juvenile hormone in insects. *Annu. Rev. Entomol.* **50**, 181-199. doi:10.1146/annurev.ento.50.071803.130356

**Blaser, H., Eisenbeiss, S., Neumann, M., Reichman-Fried, M., Thisse, B., Thisse, C. and Raz, E.** (2005). Transition from non-motile behaviour to directed migration during early PGC development in zebrafish. *J. Cell Sci.* **118**, 4027-4038. doi:10.1242/jcs.02522

**Boldajipour, B., Mahabaleshwar, H., Kardash, E., Reichman-Fried, M., Blaser, H., Minina, S., Wilson, D., Xu, Q. and Raz, E.** (2008). Control of chemokine-guided cell migration by ligand sequestration. *Cell* **132**, 463-473. doi:10.1016/j.cell.2007.12.034

**Boyle, M. and DiNardo, S.** (1995). Specification, migration and assembly of the somatic cells of the Drosophila gonad. *Development* **121**, 1815-1825.

**Burnett, C. and Howard, K.** (2003). Fly and mammalian lipid phosphate phosphatase isoforms differ in activity both in vitro and in vivo. *EMBO Rep.* **4**, 793-799. doi:10.1038/sj.embor.embor900

**Cai, D. and Montell, D. J.** (2014). Diverse and dynamic sources and sinks in gradient formation and directed migration. *Curr. Opin. Cell Biol.* **30**, 91-98. doi:10.1016/j.ceb.2014.06.009

**Coudreuse, D. Y. M., Roël, G., Betist, M. C., Destrée, O. and Korswagen, H. C.** (2006). Wnt gradient formation requires retromer function in Wnt-producing cells. *Science* **312**, 921-924. doi:10.1126/science.1124856

**Deshpande, G. and Schedl, P.** (2005). HMGCoA reductase potentiates hedgehog signaling in Drosophila melanogaster. *Dev. Cell* **9**, 629-638. doi:10.1016/j.devcel.2005.09.014

**Deshpande, G., Swanhart, L., Chiang, P. and Schedl, P.** (2001). Hedgehog signaling in germ cell migration. *Cell* **106**, 759-769. doi:10.1016/S0092-8674(01)00488-3

**Deshpande, G., Zhou, K., Wan, J. Y., Friedrich, J., Jourjine, N., Smith, D. and Schedl, P.** (2013). The hedgehog pathway gene shifted functions together with the hmgcr-dependent isoprenoid biosynthetic pathway to orchestrate germ cell migration. *PLoS Genet.* **9**, e1003720. doi:10.1371/journal.pgen.1003720

**Dickson, B. J. and Gilestro, G. F.** (2006). Regulation of commissural axon pathfinding by slit and its Robo receptors. *Annu. Rev. Cell Dev. Biol.* **22**, 651-675. doi:10.1146/annurev.cellbio.21.090704.151234

**Duchek, P. and Rørth, P.** (2001). Guidance of cell migration by EGF receptor signaling during Drosophila oogenesis. *Science* **291**, 131-133. doi:10.1126/science.291.5501.131
**Duchek, P., Somogyi, K., Jékely, G., Beccari, S. and Rørth, P.** (2001). Guidance of cell migration by the Drosophila PDGF/VEGF receptor. *Cell* **107**, 17-26. doi:10.1016/S0092-8674(01)00502-5
**Dunin-Borkowski, O. M. and Brown, N. H.** (1995). Mammalian CD2 is an effective heterologous marker of the cell surface in Drosophila. *Dev. Biol.* **168**, 689-693. doi:10.1006/dbio.1995.1115
**Eaton, S.** (2008). Multiple roles for lipids in the Hedgehog signalling pathway. *Nat. Rev. Mol. Cell Biol.* **9**, 437-445. doi:10.1038/nrm2414
**Farin, H. F., Jordens, I., Mosa, M. H., Basak, O., Korving, J., Tauriello, D. V. F., de Punder, K., Angers, S., Peters, P. J., Maurice, M. M. et al.** (2016). Visualization of a short-range Wnt gradient in the intestinal stem-cell niche. *Nature* **530**, 340-343. doi:10.1038/nature16937
**Fietz, M. J., Jacinto, A., Taylor, A. M., Alexandre, C. and Ingham, P. W.** (1995). Secretion of the amino-terminal fragment of the hedgehog protein is necessary and sufficient for hedgehog signalling in Drosophila. *Curr. Biol.* **5**, 643-650. doi:10.1016/S0960-9822(95)00129-1
**Garcia-Murillas, I., Pettitt, T., Macdonald, E., Okkenhaug, H., Georgiev, P., Trivedi, D., Hassan, B., Wakelam, M. and Raghu, P.** (2006). lazaro encodes a lipid phosphate phosphohydrolase that regulates phosphatidylinositol turnover during Drosophila phototransduction. *Neuron* **49**, 533-546. doi:10.1016/j.neuron.2006.02.001
**Hanyu-Nakamura, K., Kobayashi, S. and Nakamura, A.** (2004). Germ cell-autonomous Wunen2 is required for germline development in Drosophila embryos. *Development* **131**, 4545-4553. doi:10.1242/dev.01321
**Harvey, S. A. and Smith, J. C.** (2009). Visualisation and quantification of morphogen gradient formation in the zebrafish. *PLoS Biol.* **7**, e1000101. doi:10.1371/journal.pbio.1000101
**Ile, K. E., Tripathy, R., Goldfinger, V. and Renault, A. D.** (2012). Wunen, a Drosophila lipid phosphate phosphatase, is required for septate junction-mediated barrier function. *Development* **139**, 2535-2546. doi:10.1242/dev.077289
**Jaglarz, M. K. and Howard, K. R.** (1994). Primordial germ cell migration in Drosophila melanogaster is controlled by somatic tissue. *Development* **120**, 83-89.
**Kassmer, S. H., Rodriguez, D., Langenbacher, A. D., Bui, C. and De Tomaso, A. W.** (2015). Migration of germline progenitor cells is directed by sphingosine-1-phosphate signalling in a basal chordate. *Nat. Commun.* **6**, 8565. doi:10.1038/ncomms9565
**LeBlanc, M. G. and Lehmann, R.** (2017). Domain-specific control of germ cell polarity and migration by multifunction Tre1 GPCR. *J. Cell Biol.* **216**, 2945-2958. doi:10.1083/jcb.201612053
**Lécuyer, E., Parthasarathy, N. and Krause, H. M.** (2008). Fluorescent in situ hybridization protocols in Drosophila embryos and tissues. *Methods Mol. Biol.* **420**, 289-302. doi:10.1007/978-1-59745-583-1_18
**Lee, J. J., von Kessler, D. P., Parks, S. and Beachy, P. A.** (1992). Secretion and localized transcription suggest a role in positional signaling for products of the segmentation gene hedgehog. *Cell* **71**, 33-50. doi:10.1016/0092-8674(92)90264-D
**Lehmann, R. and Tautz, D.** (1994). In situ hybridization to RNA. *Methods Cell Biol.* **44**, 575-598. doi:10.1016/S0091-679X(08)60933-4
**Li, G., Adesnik, H., Li, J., Long, J., Nicoll, R. A., Rubenstein, J. L. R. and Pleasure, S. J.** (2008). Regional distribution of cortical interneurons and development of inhibitory tone are regulated by Cxcl12/Cxcr4 signaling. *J. Neurosci.* **28**, 1085-1098. doi:10.1523/JNEUROSCI.4602-07.2008
**McDowell, N., Gurdon, J. B. and Grainger, D. J.** (2001). Formation of a functional morphogen gradient by a passive process in tissue from the early Xenopus embryo. *Int. J. Dev. Biol.* **45**, 199-207.
**Mukherjee, A., Neher, R. A. and Renault, A. D.** (2013). Quantifying the range of a lipid phosphate signal in vivo. *J. Cell Sci.* **126**, 5453-5464. doi:10.1242/jcs.136176
**Nellen, D., Burke, R., Struhl, G. and Basler, K.** (1996). Direct and long-range action of a DPP morphogen gradient. *Cell* **85**, 357-368. doi:10.1016/S0092-8674(00)81114-9
**Paksa, A., Bandemer, J., Hoeckendorf, B., Razin, N., Tarbashevich, K., Minina, S., Meyen, D., Biundo, A., Leidel, S. A., Peyrieras, N. et al.** (2016). Repulsive cues combined with physical barriers and cell-cell adhesion determine progenitor cell positioning during organogenesis. *Nat. Commun.* **7**, 11288. doi:10.1038/ncomms11288
**Renault, A. D., Sigal, Y. J., Morris, A. J. and Lehmann, R.** (2004). Soma-germ line competition for lipid phosphate uptake regulates germ cell migration and survival. *Science* **305**, 1963-1966. doi:10.1126/science.1102421
**Renault, A. D., Ricardo, S., Kunwar, P. S., Santos, A., Starz-Gaiano, M., Stein, J. A. and Lehmann, R.** (2009). Hedgehog does not guide migrating Drosophila germ cells. *Dev. Biol.* **328**, 355-362. doi:10.1016/j.ydbio.2009.01.042
**Renault, A. D., Kunwar, P. S. and Lehmann, R.** (2010). Lipid phosphate phosphatase activity regulates dispersal and bilateral sorting of embryonic germ cells in Drosophila. *Development* **137**, 1815-1823. doi:10.1242/dev.046110
**Reuter, R.** (1994). The gene serpent has homeotic properties and specifies endoderm versus ectoderm within the Drosophila gut. *Development* **120**, 1123-1135.
**Ricardo, S. and Lehmann, R.** (2009). An ABC transporter controls export of a Drosophila germ cell attractant. *Science* **323**, 943-946. doi:10.1126/science.1166239
**Roberts, R., Sciorra, V. A. and Morris, A. J.** (1998). Human type 2 phosphatidic acid phosphohydrolases. Substrate specificity of the type 2a, 2b, and 2c enzymes and cell surface activity of the 2a isoform. *J. Biol. Chem.* **273**, 22059-22067. doi:10.1074/jbc.273.34.22059
**Sano, H., Renault, A. D. and Lehmann, R.** (2005). Control of lateral migration and germ cell elimination by the Drosophila melanogaster lipid phosphate phosphatases Wunen and Wunen 2. *J. Cell Biol.* **171**, 675-683. doi:10.1083/jcb.200506038
**Seifert, J. R. K. and Lehmann, R.** (2012). Drosophila primordial germ cell migration requires epithelial remodeling of the endoderm. *Development* **139**, 2101-2106. doi:10.1242/dev.078949
**Shellard, A. and Mayor, R.** (2016). Chemotaxis during neural crest migration. *Semin. Cell Dev. Biol.* **55**, 111-118. doi:10.1016/j.semcdb.2016.01.031
**Sigal, Y. J., Mcdermott, M. I. and Morris, A. J.** (2005). Integral membrane lipid phosphatases/phosphotransferases: common structure and diverse functions. *Biochem. J.* **387**, 281-293. doi:10.1042/BJ20041771
**Sonnenblick, B. P.** (1941). Germ cell movements and sex differentiation of the gonads in the Drosophila embryo. *Proc. Natl. Acad. Sci. USA* **27**, 484-489. doi:10.1073/pnas.27.10.484
**Starz-Gaiano, M., Cho, N. K., Forbes, A. and Lehmann, R.** (2001). Spatially restricted activity of a Drosophila lipid phosphatase guides migrating germ cells. *Development* **128**, 983-991.
**van den Heuvel, M., Nusse, R., Johnston, P. and Lawrence, P. A.** (1989). Distribution of the wingless gene product in Drosophila embryos: a protein involved in cell-cell communication. *Cell* **59**, 739-749. doi:10.1016/0092-8674(89)90020-2
**Van Doren, M., Broihier, H. T., Moore, L. A. and Lehmann, R.** (1998). HMG-CoA reductase guides migrating primordial germ cells. *Nature* **396**, 466-469. doi:10.1038/24871
**Williams, P. H., Hagemann, A., González-Gaitán, M. and Smith, J. C.** (2004). Visualizing long-range movement of the morphogen Xnr2 in the Xenopus embryo. *Curr. Biol.* **14**, 1916-1923. doi:10.1016/j.cub.2004.10.020
**Yu, S. R., Burkhardt, M., Nowak, M., Ries, J., Petrášek, Z., Scholpp, S., Schwille, P. and Brand, M.** (2009). Fgf8 morphogen gradient forms by a source-sink mechanism with freely diffusing molecules. *Nature* **461**, 533-536. doi:10.1038/nature08391
**Zecca, M., Basler, K. and Struhl, G.** (1996). Direct and long-range action of a wingless morphogen gradient. *Cell* **87**, 833-844. doi:10.1016/S0092-8674(00)81991-1
**Zhang, N., Zhang, J., Cheng, Y. and Howard, K.** (1996). Identification and genetic analysis of wunen, a gene guiding Drosophila melanogaster germ cell migration. *Genetics* **143**, 1231-1241.
**Zhang, N., Zhang, J., Purcell, K. J., Cheng, Y. and Howard, K.** (1997). The Drosophila protein Wunen repels migrating germ cells. *Nature* **385**, 64-67. doi:10.1038/385064a0

Fig. S1

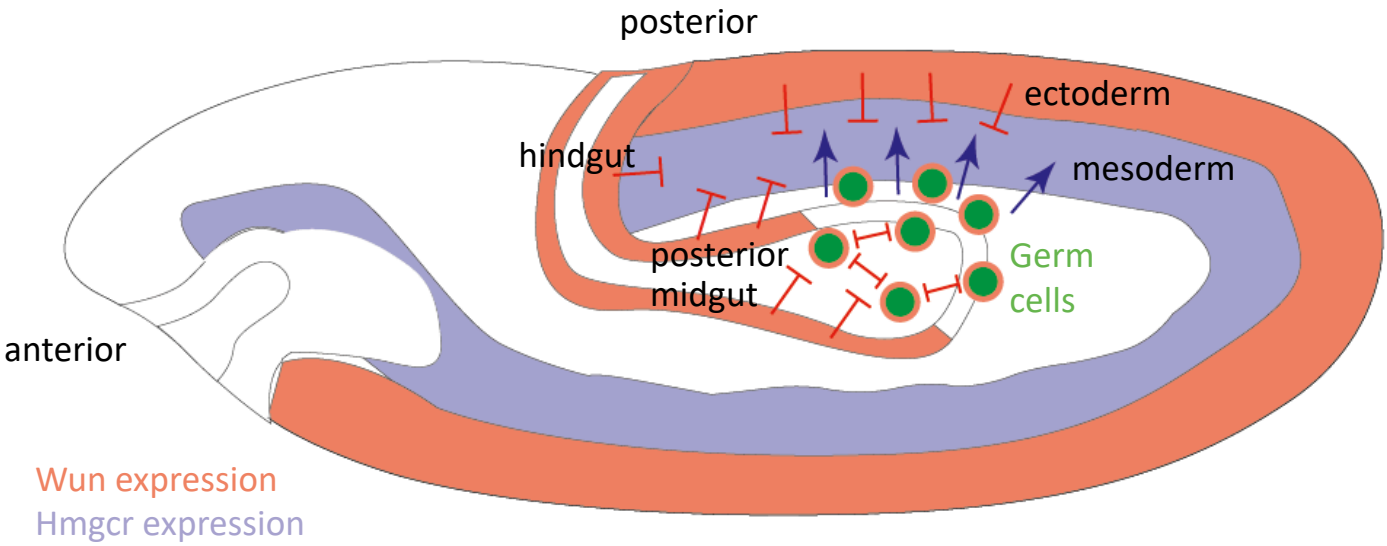


**Figure S1. Complementary expression patterns of Hmgcr and Wun guide germ cells to the SGPs.**

Hmgcr expression (light blue) in the mesoderm and later just in the SGPs, which are derived from the mesoderm, is responsible for attracting (blue arrows) the germ cells (green). Wunen expression (light red) in regions of the ectoderm and posterior midgut repels germ cells (red bar-headed lines). Wunen expression on germ cells themselves causes mutual repulsion leading to germ cell dispersal.

Fig. S2

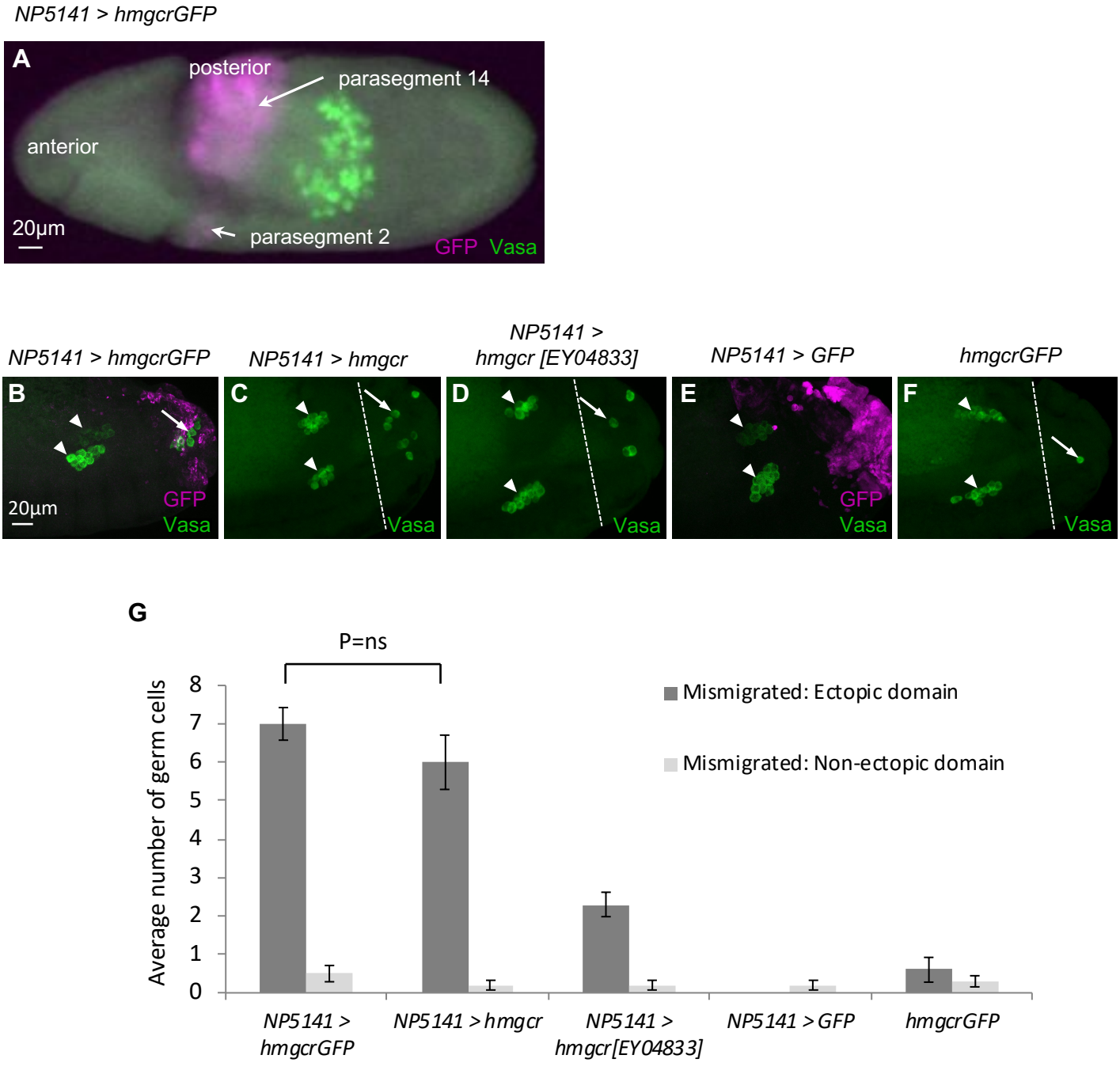

**Figure S2. GFP tagged Hmgcr is functional.**

(A) Maximum intensity projection of a lateral view of a *NP5141Gal4/+; UAS hmgcrGFP/+* stage 10 embryo, fluorescently stained with antibodies against Vasa to label the germ cells (green) and GFP to visualize the *hmgcrGFP* expression (magenta). *NP5141*-driven transgene expression is observed in parasegments 2 and 14.

(B-F) Maximum intensity projections of lateral views of stage 14 embryos, fluorescently stained with antibodies against Vasa (green, germ cells) and GFP (magenta, ectopic domain) (B, E only) of the genotypes: *NP5141Gal4/+; UAShmgcrGFP/+* (B), *NP5141Gal4/+; UAShmgcr/+* (C), *NP5141Gal4/+; hmgcr$^{EY04833}$/+* (D), *NP5141Gal4/UASGFP* (E) and *UAShmgcrGFP/UAShmgcrGFP* (F). Arrows indicate mismigrated germ cells located in the ectopic domain, arrowheads indicate the embryonic gonads. Estimate of boundary of ectopic domain indicated with dashed white line (C, D, and F).

(G) Graph showing the mean ± s.e.m number of mismigrated germ cells (defined as being outside of the gonad cluster) located either within or outside of the ectopic domain in stage 14 embryos. n=10 embryos scored per genotype. A Student's t-test (two tailed) indicates there was no significance difference between the number of ectopically attracted germ cells when using untagged and GFP tagged *hmgcr* ($P$>0.05, ns).

Fig. S3

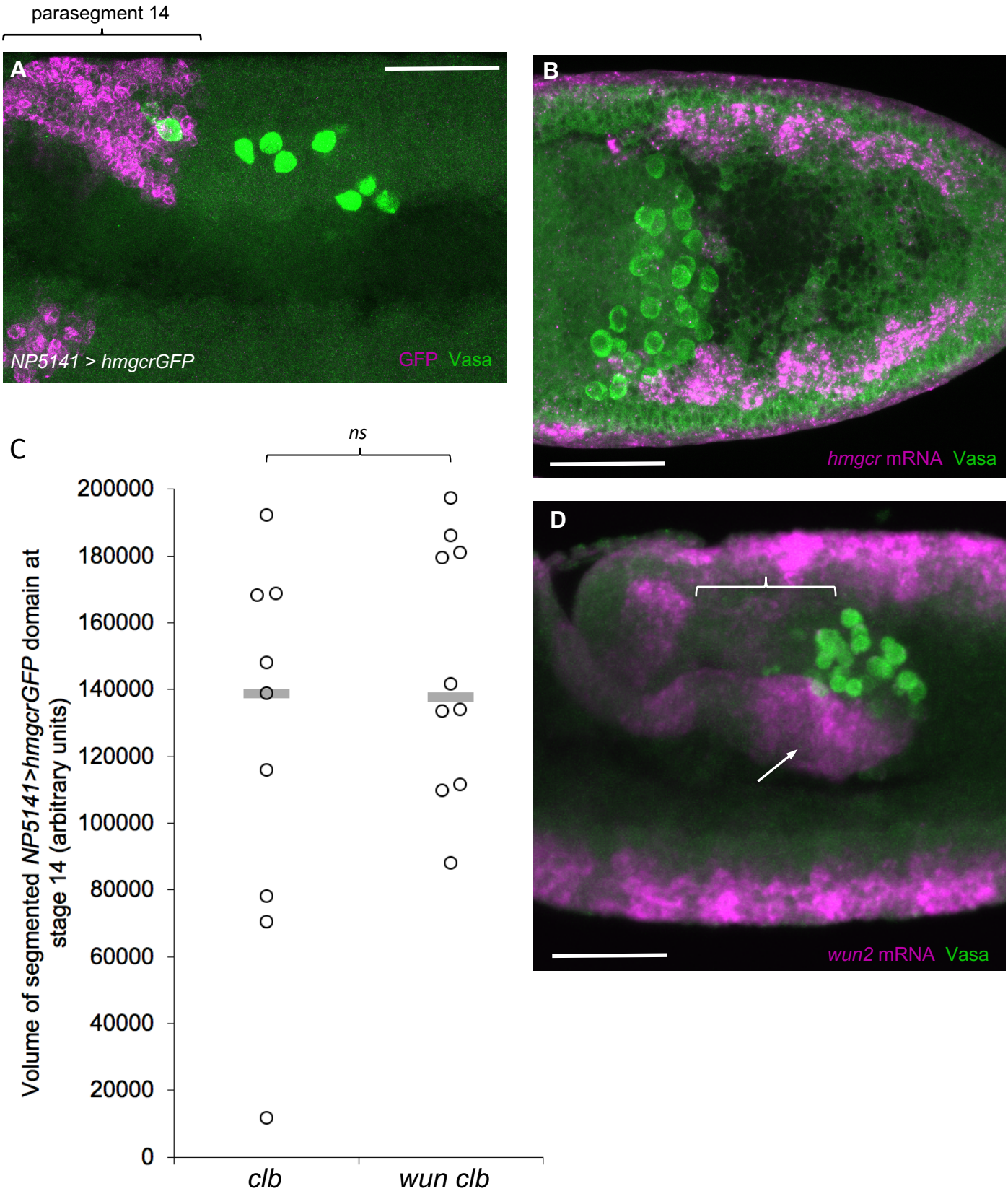

**Figure S3. Size of ectopic and endogenous *hmgcr* domains.**

(A-B) Images used to estimate the number of *hmgcr* endogenously and ectopically expressing cells**.** (A) Lateral view of a maximum intensity projection of a *NP5141Gal4/+; UAS hmgcrGFP/+* stage 10 embryo, fluorescently stained with antibodies against Vasa to label the germ cells (green) and GFP to visualise the ectopic domain (magenta). The number of *hmgcr* expressing cells in parasegment 14 was scored manually.

(B) Maximum intensity projection of a dorsal view of a wild type embryo at stage 10 fluorescently stained with antibodies against Vasa to label the germ cells (green) and a *hmgcr* RNA probe to visualise *hmgcr* expression (magenta). The number of *hmgcr* expressing cells in the mesoderm that overlies the germ cells was scored manually.

(C) Volume of segmented *hmgcrGFP* expressing region in stage 14 embryos in both *clb* and *wun clb* double mutants showing that it is not altered in a *wun* null background (Student's t-test (two tailed) $P>0.05$, ns). Median values are indicated by a grey bar.

(D) Maximum intensity projection of a lateral view of a wild type embryo at stage 10 fluorescently stained with antibodies against Vasa to label the germ cells (green) and a *wun2* RNA probe to visualise *wun2* expression (magenta) showing that *wun2* is expressed at the same stage as *hmgcr* (shown in B) and that there is no *wun2* expression between the germ cells and parasegment 14 (curly bracket). Arrow indicates *wun2* expression in the posterior midgut. Scale bars are 50 µm.

Fig. S4

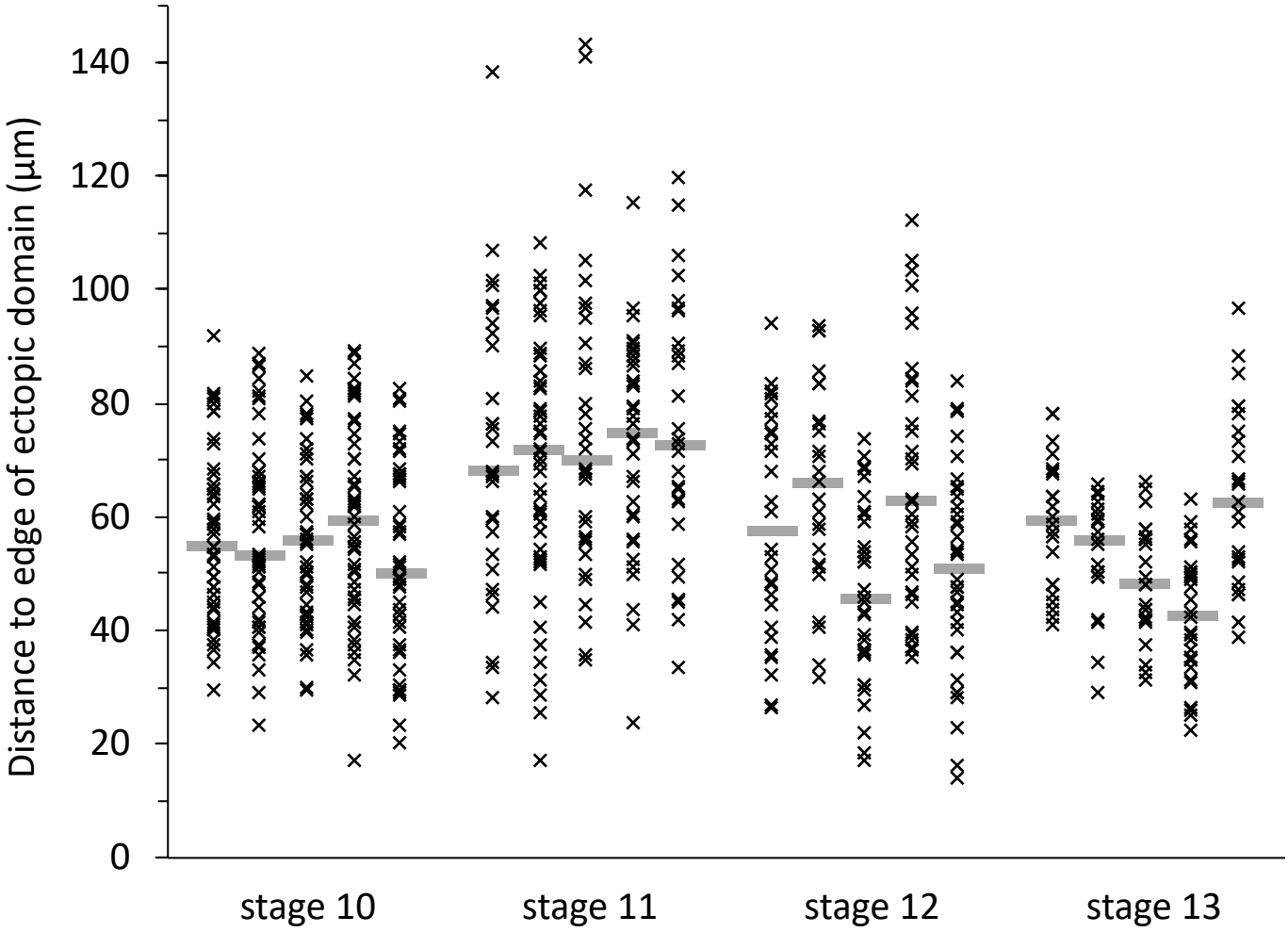


**Figure S4. Germ cells remain at a similar distance to the NP5141 ectopic domain throughout embryogenesis.**

Graph showing distance of all germ cells to the closest point of a GFP expressing NP5141 ectopic domain in a wild type background (*NP5141Gal4/UASGFP* embryos). 5 embryos of each stage are shown. Median value for each embryo is indicated by a gray bar.

Fig. S5

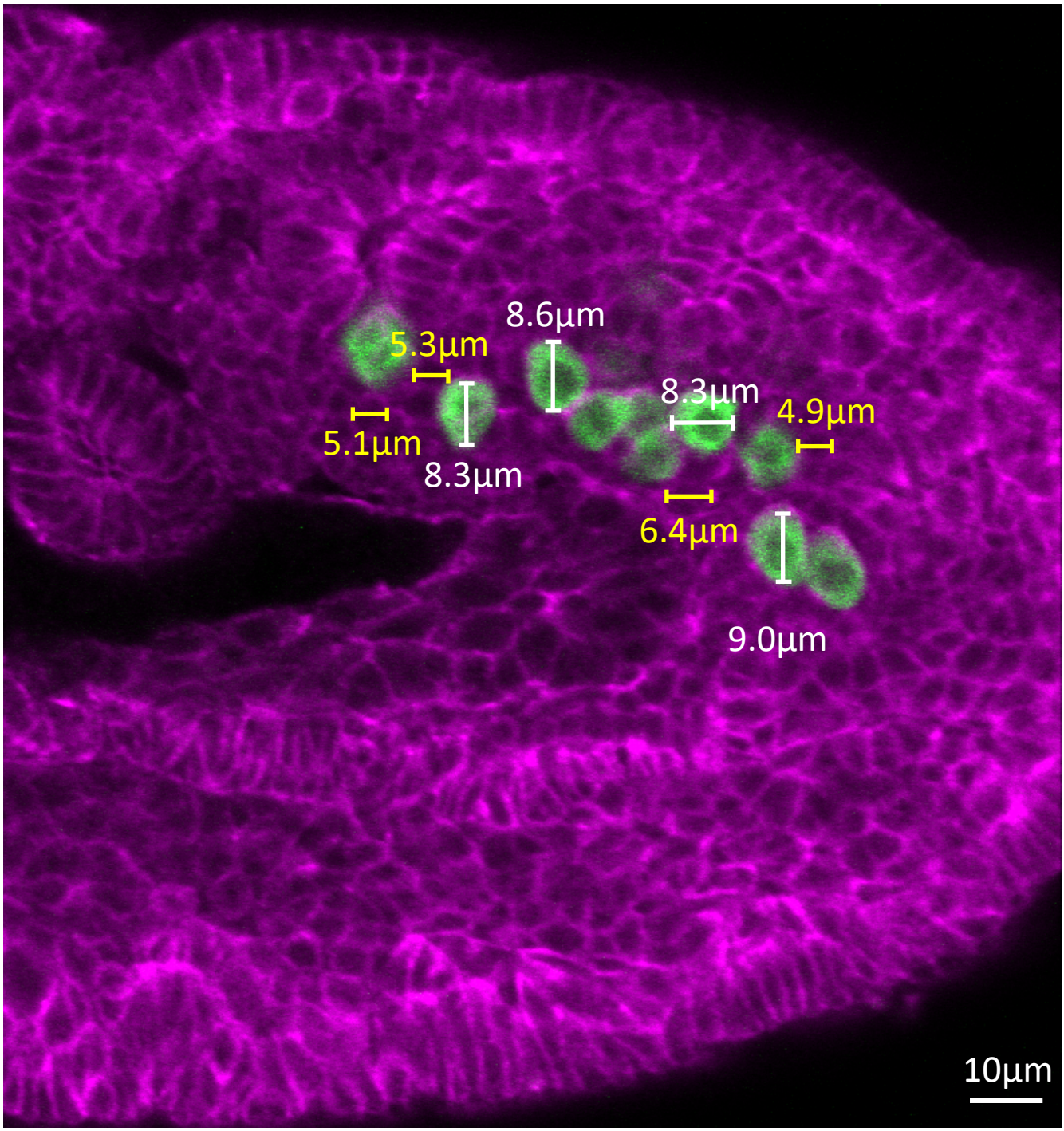


**Figure S5. Size of mesodermal and germ cells.**

Lateral view of stage 12 embryo fluorescently stained with antibodies against Vasa to label the germ cells (green) and α-spectrin to visualise plasma membranes (magenta). Diameters of selected germ cells (white bars) and mesodermal cells (yellow bars) are indicated.

Fig. S6

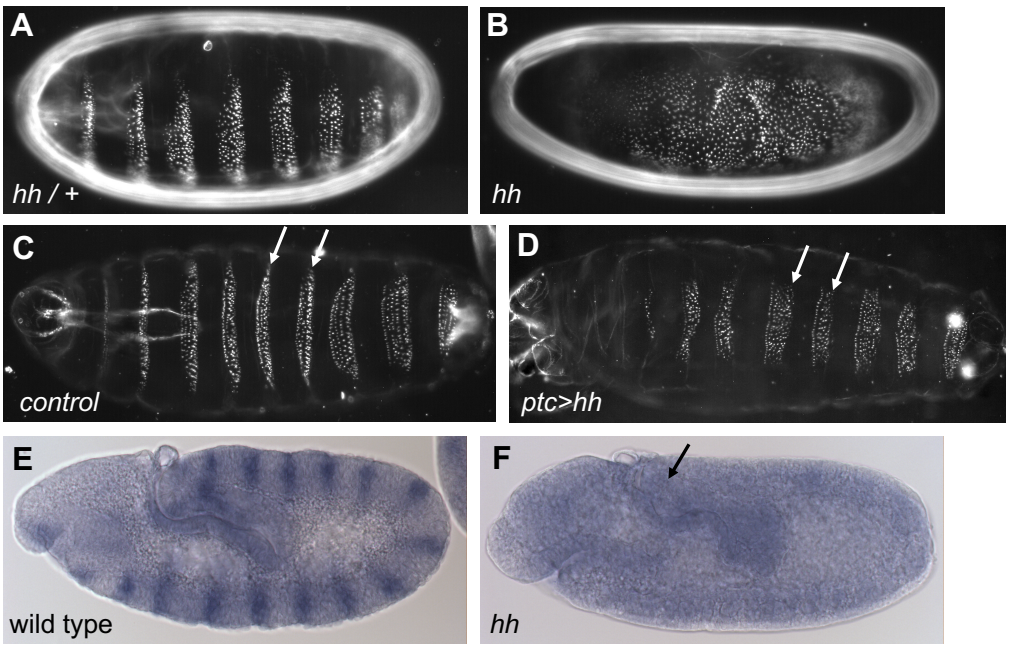


**Figure S6. Verification of *hedgehog* mutant and over-expression stocks.**

(A-D) Darkfield images of cuticle preparations. Late embryos from a *UAShmgcrGFP hh$^{AC}$/TM3ftz>lacZ* stock with heterozygous sibling (A) exhibiting a wild type denticle pattern and homozygous *UAShmgcrGFP hh$^{AC}$* mutant embryos exhibiting a pattern characteristic of *hh* null mutants (B). (C-D) Control larvae (E) and larvae over-expressing *hh* using a *patched* Gal4 driver (F), the latter demonstrating loss of the longer rows of posterior denticles from each belt (arrows in C and D) demonstrating functional *hh* over-expression.

(E-F) *In situ* hybridisation using a *hh* probe in wild type (E) and *hh$^{AC}$* mutant (F) stage 10 embryos showing that maternal *hh* message is not evident at stage 10 in parasegment 14 (arrow).

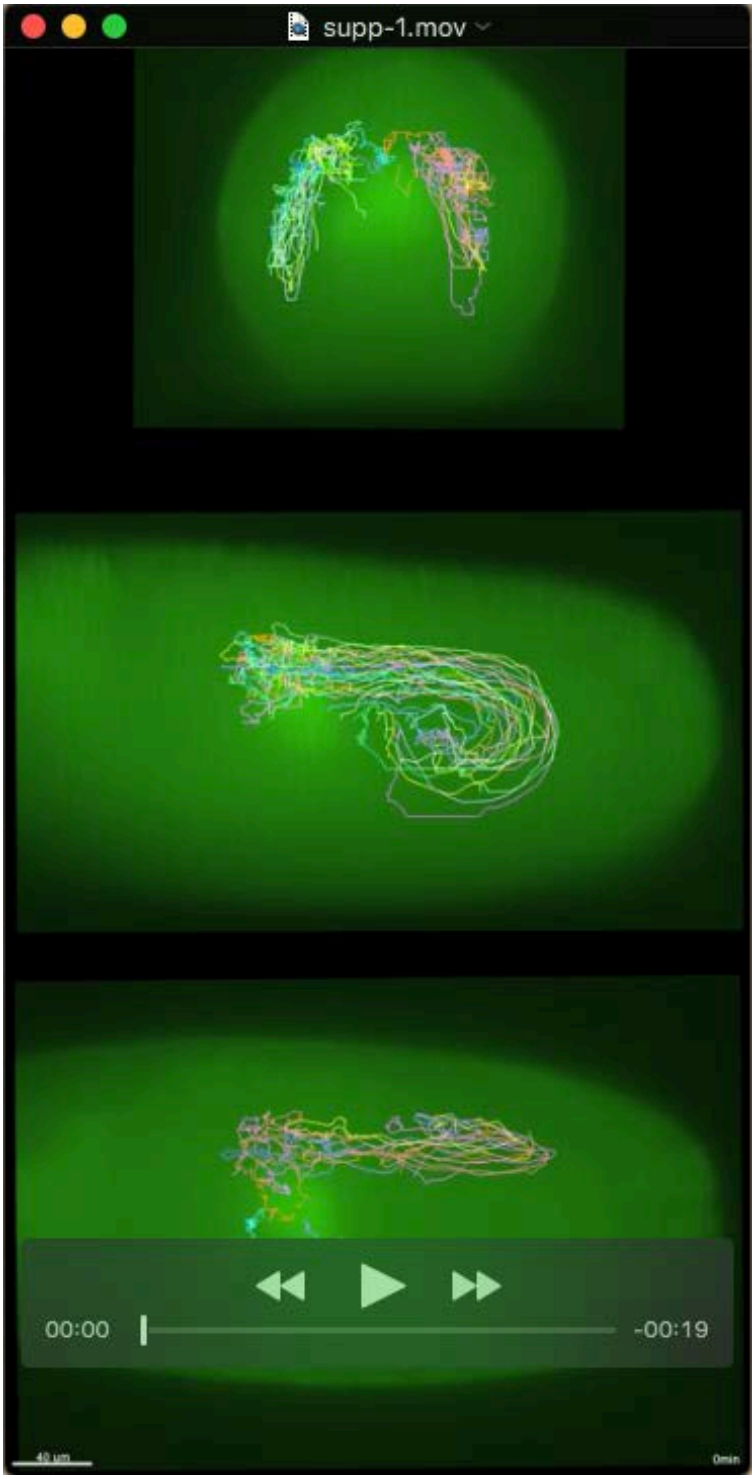


**Movie 1**
Relates to Figure 5A.

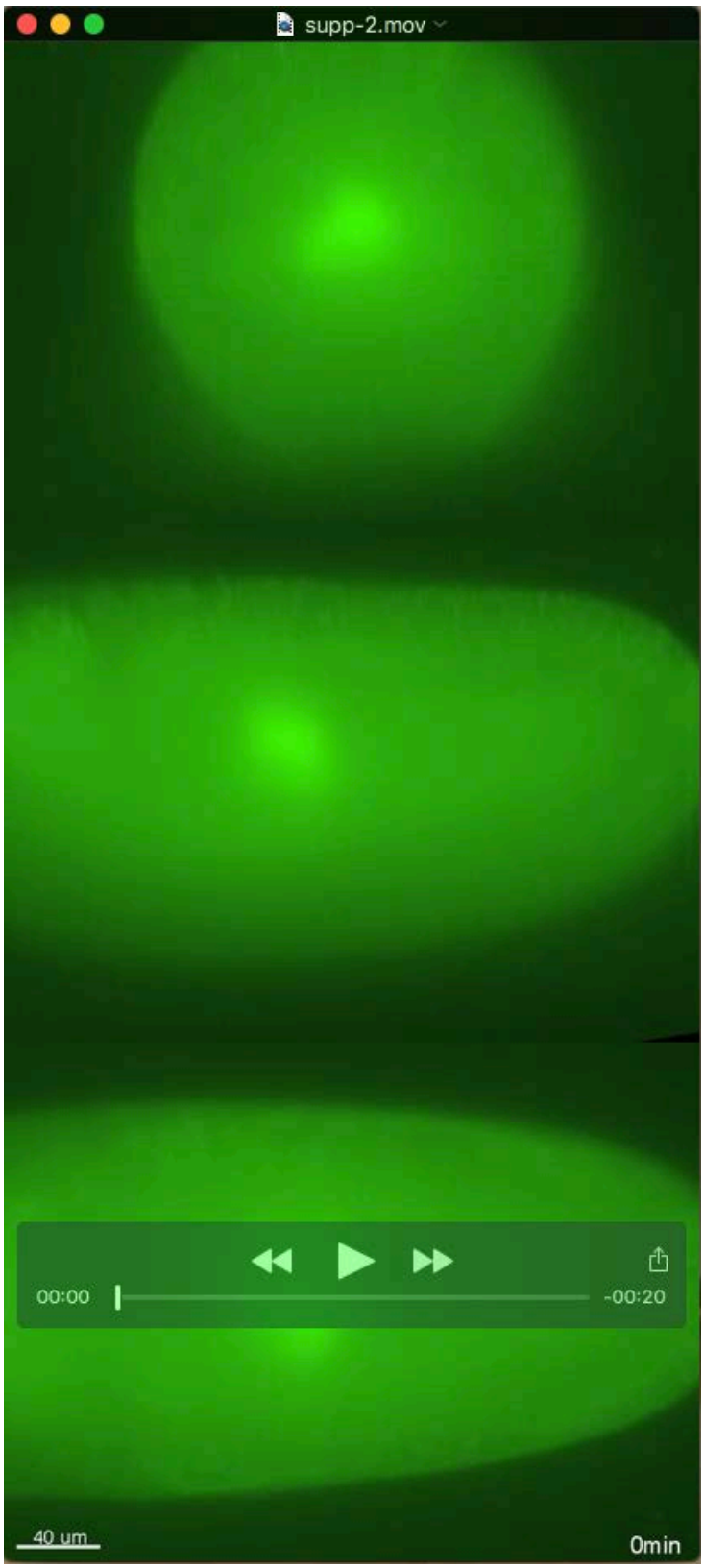


**Movie 2**
Relates to Figure 5A (tracking removed)

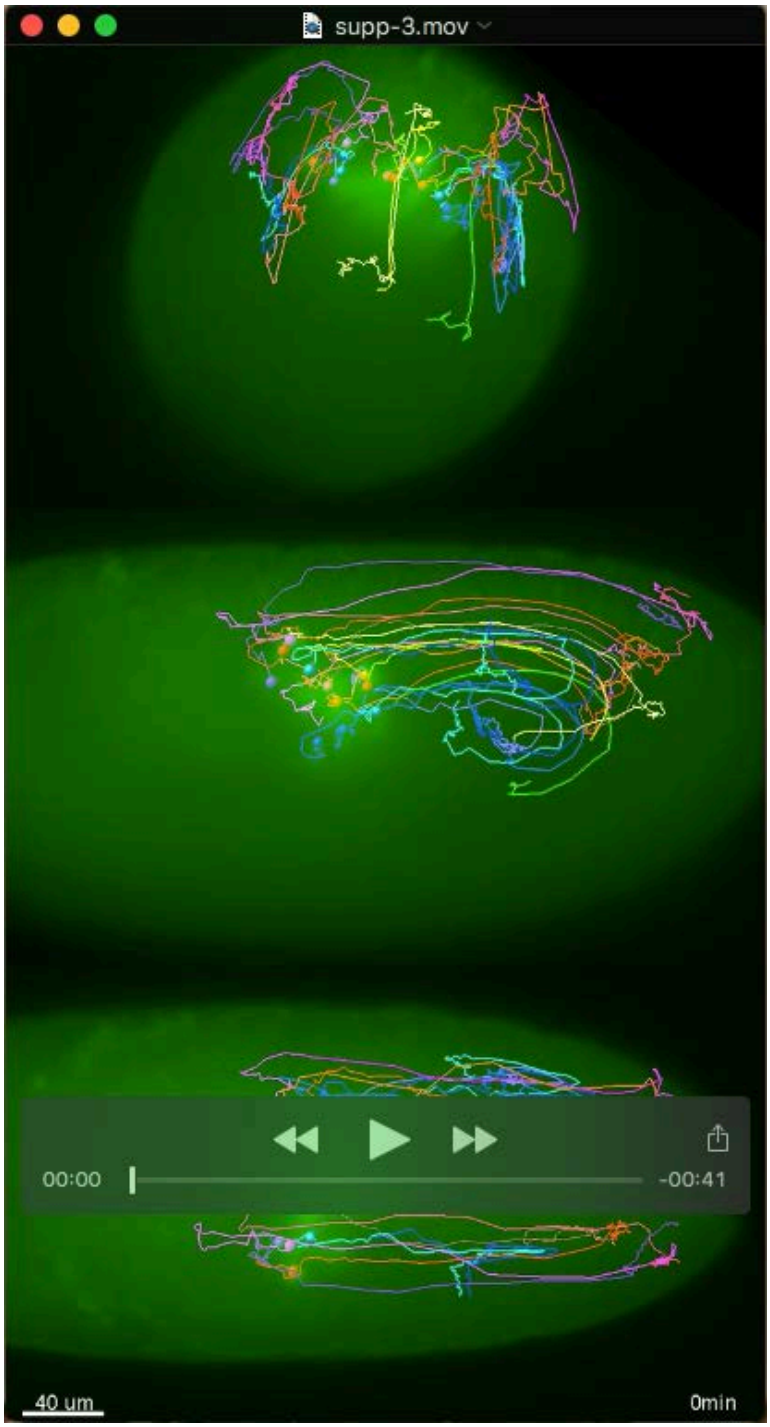


**Movie 3**
Relates to Figure 5B.

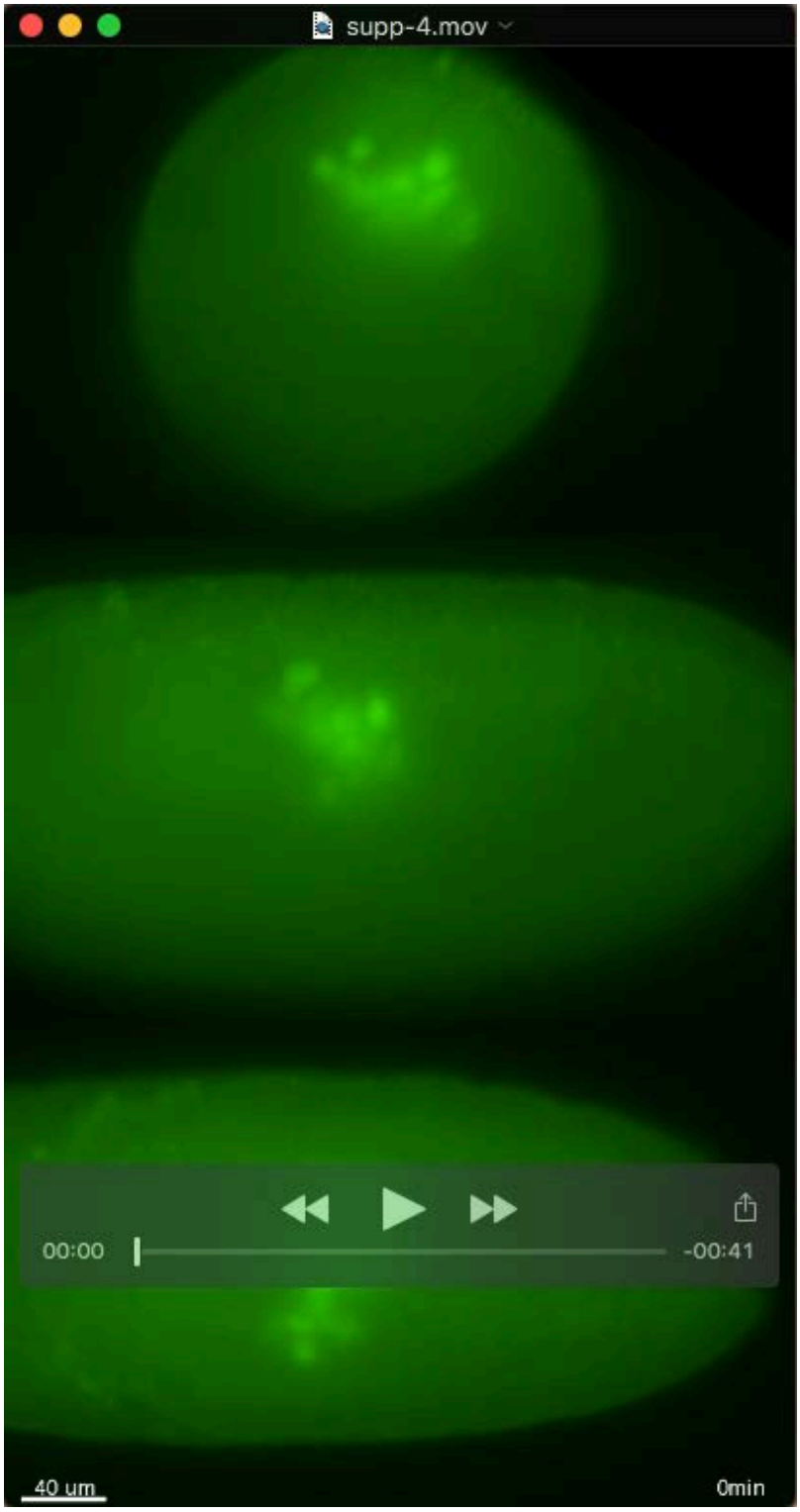


**Movie 4**
Relates to Figure 5B (tracking removed)